HHS Public Access

Author manuscript

Nature. Author manuscript; available in PMC 2014 November 15.

Published in final edited form as:

Nature. 2014 May 15; 509(7500): 337–341. doi:10.1038/nature13309.

c-kit+ Cells Minimally Contribute Cardiomyocytes to the Heart

Jop H. van Berlo[1,2,*], **Onur Kanisicak**[1,*], **Marjorie Maillet**[1], **Ronald J. Vagnozzi**[1], **Jason Karch**[1], **Suh-Chin J. Lin**[1], **Ryan C. Middleton**[3], **Eduardo Marbán**[3], and **Jeffery D. Molkentin**[1,4]

[1]Department of Pediatrics, Cincinnati Children's Hospital Medical Center, Cincinnati, OH USA

[2]Department of Medicine, division of Cardiology, Lillehei Heart Institute, University of Minnesota, Minneapolis, MN USA

[3]Cedars-Sinai Heart Institute, 8700 Beverly Blvd., Los Angeles, CA USA

[4]Howard Hughes Medical Institute, Cincinnati Children's Hospital Medical Center, Cincinnati, OH USA

Abstract

If and how the heart regenerates after an injury event is highly debated. c-kit-expressing cardiac progenitor cells have been reported as the primary source for generation of new myocardium after injury. Here we generated two genetic approaches in mice to examine if endogenous c-kit$^+$ cells contribute differentiated cardiomyocytes to the heart during development, with aging or after injury in adulthood. A cDNA encoding either Cre recombinase or a tamoxifen inducible MerCreMer chimeric protein was targeted to the *Kit* locus in mice and then bred with reporter lines to permanently mark cell lineage. Endogenous c-kit$^+$ cells did produce new cardiomyocytes within the heart, although at a percentage of ≈0.03% or less, and if a preponderance towards cellular fusion is considered, the percentage falls below ≈0.008%. In contrast, c-kit$^+$ cells amply generated cardiac endothelial cells. Thus, endogenous c-kit$^+$ cells can generate cardiomyocytes within the heart, although likely at a functionally insignificant level.

Correspondence: Jeff.Molkentin@cchmc.org.
*These authors contributed equally to this work

Supplementary Information:
Discussion
Methods
Extended Data Figures 1–9
Supplementary Table 1

Author Contributions:
J.D.M., J.H.v.B., O.K., M.M., S-C.J.L., and R.J.V., designed the experiments. S-C.J.L., designed the Kit allele targeting construct and targeted mice. J.H.v.B., and O.K., designed the breeding, performed histological experiments and animal procedures. R.J.V., performed the quantitative PCR assays. M.M., performed immunohistochemistry. J.K., performed cell culture experiments. E.M. and R.C.M designed and conducted the independent verification immunohistochemistry with blinded samples. J.D.M., wrote the manuscript.

Conflict of Interest or Competing Financial Interest:
None

Introduction

The adult mammalian heart was originally proposed to be essentially incapable of renewal after injury or with aging; although some recent studies have shown that the heart is capable of new cardiomyocyte formation with varying degrees of regenerative potential [1]. The concept that stem cells are the source for cardiomyocyte regeneration arose from initial observations in which bone marrow derived c-kit$^+$ hematopoietic stem cells (HSCs) showed restoration of the myocardium after infarction injury when given exogenously [2]. However, subsequent studies demonstrated that HSCs possessed essentially no ability to make cardiomyocytes, calling into question these earlier reports [3,4], at which time the field shifted to a focus on endogenous c-kit$^+$ cardiac progenitor cells (CPCs) residing within the myocardium [5]. Such cells isolated from the rat heart were reported to differentiate into cardiomyocytes, smooth muscle cells and endothelial cells, even after clonal derivation, and when injected into the infarct region they produced substantial new myocardium [6]. Mouse and human c-kit$^+$-CPCs were also isolated and marked, and after injection into an infarcted mouse heart, were shown to generate substantial levels of labeled cardiomyocytes, capillaries and fibroblasts [7]. More recently, resident c-kit$^+$ CPCs were reported to be both necessary and sufficient for complete repair and functional restoration of the myocardium after isoproterenol induced cardiomyocyte killing, while bone marrow derived c-kit$^+$ cells had no regenerative effect [8]. However, other studies with adult cardiac resident c-kit$^+$ cells have reported the opposite; that these cells do not possess the ability to generate cardiomyocytes in vivo [4,9,10]. To address ongoing controversy, we generated mice in which the *Kit* locus was used for lineage tracing analysis to examine if and how frequently c-kit$^+$ cells generate cardiomyocytes *in vivo*.

c-kit$^+$ contribution to the growing heart

The *Kit* locus was targeted with a cDNA encoding Cre recombinase fused to an internal ribosome entry sequence (IRES) to concurrently express enhanced green fluorescent protein (eGFP) tagged with a nuclear localization signal (nls) (Fig. 1a). These Kit$^{+/Cre}$ mice were bred to LoxP site-dependent *Rosa26-CAG-loxP-STOP-loxP-eGFP* (R-GFP) reporter mice to irreversibly mark any cell that previously or currently expresses this *Kit* locus (Fig. 1a). Four to eight weeks after birth the fidelity of the genetic system was assessed in comparison with known domains of c-kit protein expression, such as melanocytes of the skin, Leydig cells in the testis, interstitial cells of the intestine and wide areas of the spleen, all of which showed eGFP cellular labeling (Fig. 1b, Extended Data Fig. 1a) [11–13]. In bone marrow, 83% of the c-kit antibody detected cells were eGFP$^+$ by standard FACS analysis (Fig. 1c), while imaging cytometry analysis detected coincident eGFP$^+$ expression and c-kit immunoreactivity in 88% of the bone marrow cells and 76% of the non-myocyte fraction from the heart (Fig. 1d, e). To further verify the specificity of the *Kit*-Cre allele we examined real time eGFPnls expression in the heart, ileum and skeletal muscle for coexpression of c-kit protein (antibody), which was always coincident (Fig. 1f, g, and Extended Data Fig. 1b, c). In bone marrow, 94% of the eGFP$^+$ cells were Lin$^+$, indicating a high degree of fidelity with the *Kit*-Cre allele (Extended Data Fig. 1d). In the heart c-kit antibody positive mononuclear cells were predominantly eGFP$^+$ at 4 weeks of age using the *Kit*$^{+/Cre}$ × R-GFP reporter strategy, while in testis recombination was only observed in

Leydig cells, of which >80% were eGFP$^+$ (Extended Data Fig. 1e, f). Thus, the specificity of the *Kit*-Cre allele appears identical with known regions of c-kit protein expression *in vivo*.

In an exhaustive search by histological methods across three hearts from Kit$^{+/Cre}$ mice for current eGFPnls expression at 4 weeks of age, no eGFP$^+$ cardiomyocytes or endothelial cells were identified (only mononuclear CPC-like cells were observed), strongly suggesting that the *Kit* locus is not spontaneously activated in differentiated celltypes of the heart (Fig 1f). However, in conjunction with the R-GFP reporter allele for ongoing c-kit lineage tracing, the myocardium showed many eGFP$^+$ differentiated cell types, although cardiomyocytes were very rare (Fig. 1h, i). Even more rarely, areas suggestive of cardiomyocyte clonal expansion were identified (Fig. 1i). No eGFP$^+$ cells were observed in hearts of single R-GFP mice (data not shown). To more rigorously quantify the extent of cardiomyocyte recombination-based labeling, hearts were disassociated and eGFP$^+$ cells were directly counted (Fig. 1j), revealing a level of 0.027% myocytes from the c-kit lineage (Fig. 1k). This low percentage was confirmed by PCR analysis for DNA recombination at the *Rosa26* locus from purified cardiomyocytes vs spleen (Fig. 1l).

c-kit$^+$ non-myocyte lineage analysis

Hearts of Kit$^{+/Cre}$ × R-GFP mice at 4 weeks of age were further examined to identify the remaining eGFP$^+$ non-myocytes. Examples of eGFP labeling co-incident with fibroblasts (vimentin co-labeling), endothelial cells (CD31, CD34, vWF), immune cells (CD3 and CD45), and rarely smooth muscle α-actin (αSMA) expressing cells were identified, although the most prevalent co-localizations were with CD31, CD45 or CD34 positive cells (Fig. 2a–g). Indeed, using a cocktail of antibodies for CD31, CD45, CD34 and CD3, versus sarcomeric α-actin, we were able to account for almost all eGFP$^+$ non-myocytes in the hearts of adult Kit$^{+/Cre}$ × R-GFP mice, either when analyzed from histological sections or as dissociated individual cells (Extended Data Fig. 2a–c). FACS analysis showed that 18% and 77% of the total eGFP$^+$ non-myocytes in the heart were CD45 or CD31 positive, respectively (Fig. 2h and i). Confocal microscopy analysis showed exact co-localization between eGFP$^+$ cells in the heart and CD31 protein expression, but not with NG2 staining for pericytes (Fig. 2j).

We also harvested Kit$^{+/Cre}$ × R-GFP mice at birth (P0) to analyze the contributions of c-kit$^+$ cells to the heart during embryonic and fetal development (Extended Data Fig. 3a). Control histological sections from the ileum and lung showed the expected distribution of c-kit$^+$ cells (Extended Data Fig. 3b), and the heart also showed numerous eGFP$^+$ cells throughout (Extended Data Fig. 3c). Immunohistochemical analysis of the P0 heart with a sarcomeric cardiomyocyte marker showed that nearly all of the eGFP$^+$ cells were non-myocytes, although definable cardiomyocytes were clearly present at very low levels, including rare areas of cardiomyocyte clonal expansion (Extended Data Fig. 3d–g).

c-kit$^+$ lineage tracing in adult heart

To specifically address the question of new cardiomyocyte formation within the adult heart, we generated a mouse model in which the tamoxifen inducible MerCreMer protein was targeted to the *Kit* locus (Kit$^{+/MCM}$), followed by cross breeding with the R-GFP reporter

line (Fig. 3a). To verify the fidelity of this system, $Kit^{+/MCM}$ × R-GFP mice were given tamoxifen during postnatal maturation for approximately 4 weeks followed by harvesting of tissues with known sites of c-kit expression (Extended Data Fig. 4a). $Kit^{+/MCM}$ × R-GFP mice showed ≈70% overlap in recombination-dependent eGFP expression and endogenous c-kit protein in Leydig cells of the testis (Extended Data Fig. 4b). Importantly, no $eGFP^+$ cells were observed in the absence of tamoxifen at any age examined or after myocardial infarction (MI) injury, demonstrating that the MerCreMer system does not "leak" (Extended Data Fig. 4c). $Kit^{+/MCM}$ × R-GFP mice were also given tamoxifen from day 1 through 6 months of age for continuous labeling (Fig. 3b), which produced eGFP expression in greater than 60% of bone marrow cells, but again no signal in the absence of tamoxifen (Fig. 3c–e). Histological analysis of the heart after 6 months of labeling showed rare examples of $eGFP^+$ adult cardiomyocytes and a relatively large number of non-myocytes (Fig. 3f, g). Careful analysis of the non-myocyte fraction in these hearts showed fibroblasts (rarely), smooth muscle cells (rarely), endothelial cells and immune cells, with the majority again being $CD31^+$ (Extended Data Fig. 5a–h). MI injury also doubled the number of CD31 cells that were $eGFP^+$ in the adult heart with 8 weeks of prior tamoxifen labeling (Extended Data Fig. 5h). We also conducted c-kit lineage labeling from 6–12 weeks of age, just after the postnatal developmental period (Fig. 3h). Upon disassociation of these hearts we observed 0.0055% $eGFP^+$ adult cardiomyocytes (Fig. 3i, j), confirmed as extremely low by PCR and qPCR for *Rosa26* locus recombination (Extended Data Fig. 6a, b, c).

Cardiac injury increases cellular turnover in the heart, hence we subjected $Kit^{+/MCM}$ × R-GFP mice to MI at 10 weeks of age during a 6 week tamoxifen labeling protocol (Fig. 3k and Extended Data Fig. 6d–f). The percentage of $eGFP^+$ cardiomyocytes increased to 0.016% within the heart, with more being localized to the infarct border zone (Fig. 3l, m, n). $c\text{-}kit^+$ lineage cells within the heart were also pre-labeled by giving tamoxifen only before MI injury, which again showed a very low percentage of $eGFP^+$ cardiomyocytes (Fig. 3o, p). Percentages of $eGFP^+$ cardiomyocytes in the heart during 4 weeks of isoproterenol infusion-induced injury were 0.007% (Extended Data Fig. 7a–c). These astonishingly low values of cardiomyocyte formation were independently verified using blinded heart histological sections from $Kit^{+/MCM}$ × R-GFP mice sent to an outside academic laboratory (Extended Data Fig. 8a, b, c).

Finally, we also cultured total non-myocytes from the hearts of young adult $Kit^{+/Cre}$ × R-GFP mice in the presence of dexamethasone as a means of pushing $c\text{-}kit^+$ cells with progenitor-like activity towards the cardiomyocyte lineage (Extended Data Fig. 9). The data show that $eGFP^+$, *Kit*-Cre allele expressing cells are fully capable of inducing expression of the cardiac markers GATA4, α-actinin and troponin T, suggestive of partial differentiation towards the cardiomyocyte lineage (sarcomeres were not observed).

$c\text{-}kit^+$ cells fuse in the heart

Hearts from $Kit^{+/MCM}$ × R-GFP mice showed the presence of cells from blood lineages (CD3, CD45, and CD34), which are known to have fusigenic activity with resident parenchymal cells [3,14–18]. To examine fusion we employed a genetic strategy that constitutively expresses a membrane targeted fluorescent tdTomato protein from the *Rosa26*

locus. Upon Cre-mediated recombination, tdTomato fluorescence is lost and a membrane targeted eGFP becomes expressed (abbreviated "mT/mG") (Fig. 4a). If cells fuse, both signals would be present but a *de novo* cardiomyocyte from a c-kit^{+} lineage cell would be only green. Experimentally, Kit$^{+/MCM}$ × mT/mG mice were given tamoxifen for 2 weeks (8–10 weeks of age) then 3 days later MIs, followed by harvesting at 1, 2 and 4 weeks thereafter (Fig. 4b). Control mice were harvested before MI but after tamoxifen (time 0). Percentages of total cardiomyocyte membrane-eGFP labeling, whether from fusion or not, were approximately 0.01% at all three time points after MI (Fig. 4c). While some de novo cardiomyocytes were identified in the heart (eGFP only), the majority (80–88%) retained the membrane-tdTomato label indicating that these cells likely arose by fusion (Fig. 4d, e, f). Thus, c-kit^{+} lineage cells can generate cardiomyocytes in the heart, although at ≈5-fold lower values than initially predicted.

Kit-Cre locus is not ectopically induced

One concern with the *Kit* allele-based lineage tracing approach is if this locus ever becomes activated ectopically in a cardiomyocyte, it would be wrongly ascribed as having come from a c-kit^{+} cell. It was previously shown that knock-down of the *Kit* gene results in defective progenitor cell activity in many tissues [19–22]. Indeed, hearts from *Kit*$^{w/wv}$ mice showed a dramatic reduction in resident mononuclear c-kit^{+} cells and progenitor activity [23]. Hence, *Kit* null mice should lack the ability to generate eGFP^{+} cardiomyocytes in the heart if they indeed arise from c-kit^{+} cells with progenitor-like activity, instead of having arisen from ectopic *Kit* allele induction in a rare population of differentiated cardiomyocytes.

Kit null mice were generated by placing the *Kit*-Cre allele over the *Kit*-MerCreMer allele. While these mice die at birth, viable nulls at embryonic days 16.5 and 18.5 were identified and examined (Fig. 4g, h, i). Fourteen total eGFP^{+} cardiomyocytes were counted from 4 Kit$^{+/Cre}$ × R-GFP and 1 Kit$^{+/Cre}$ × mT/mG embryos across 56 histological sections spanning the heart (Fig 4j and l). However, hearts from 2 Kit$^{MCM/Cre}$ × R-GFP and 1 Kit$^{MCM/Cre}$ × mT/mG embryos (nulls) showed lower total eGFP^{+} cells in the heart and 0 cardiomyocytes across 69 histological sections (Fig. 4i, k, m). Importantly Kit$^{MCM/Cre}$ embryos showed no c-kit protein expression confirming their null status (Fig. 4n). Taken together, these data indicate that eGFP^{+} cardiomyocytes that are lineage traced with the *Kit*-Cre allele are not due to inappropriate activation of the *Kit* gene for even a brief period of time in rare existing cardiomyocytes, but rather they either arose by transdifferentiation from c-kit^{+} lineage precursor cells or by fusion.

Discussion

The original hypothesis that c-kit^{+} cells have the ability to contribute to the cardiomyocyte compartment of the heart, as well as other cell types, is correct as determined by the lineage tracing technique used here [6]. Indeed, the observation that embryonic and postnatal labeling in the hearts of Kit$^{+/Cre}$ × R-GFP mice shows definable regions with cardiomyocyte clonal expansion strongly suggests that these c-kit^{+} cells can make cardiomyocytes *in vivo*. More importantly, loss of the *Kit* gene, which is known to compromise the progenitor and migration activity of c-kit^{+} cells, completely prevented cardiomyocyte formation from c-kit^{+}

cells. However, throughout development, with aging or with cardiac injury, the percentage of cardiomyocytes emerging from the c-kit$^+$ lineage was astonishingly low and hence highly unlikely to ever significantly impact cardiac function. The mT/mG detection system also supported the existence of *de novo* cardiomyocyte formation in the adult heart from the c-kit$^+$ lineage but at ≈5-fold lower levels than initially quantified due to prevalent cellular fusion events.

Exogenous c-kit$^+$ cells are currently being used to treat post-MI heart failure patients, and early results have shown small, albeit significant functional improvements in the heart [24]. However, our results suggest that the potential benefit of injecting c-kit$^+$ cells into the hearts of patients is unlikely attributable to new cardiomyocyte formation, hence caution is warranted until the mechanisms in play are better defined, or until we are able to dramatically enhance the cardiogenic potential of these cells (see Supplemental Discussion).

METHODS SUMMARY

The *Kit* allele was targeted in SV129 embryonic stem (ES) cells to express either Cre recombinase alone or a tamoxifen-inducible Cre recombinase referred to as MerCreMer. Hemizygous targeted mice were crossed with FVB.Cg-*Gt(ROSA)26Sor*$^{tm1(CAG-lacZ,EGFP)Glh}$/J (previously modified by cross-breeding to B6(C3)-Tg(Pgk1-FLPo)10Sykr/J) or B6.129(Cg)-*Gt(ROSA)26Sor*$^{tm4(ACTB-tdTomato,-EGFP)Luo}$/J. Tissue from these mice were subjected to histological analysis and immunohistochemistry at multiple ages and after select treatments. Antibodies used are shown in Supplemental Table 1 (See online supplement for full Methods).

Methods

Mice

All experiments involving mice were approved by the Institutional Animal Care and Use Committee (IACUC) at Cincinnati Children's Hospital. No human subjects or human material was used. Targeted *Kit*-Cre-IRES-eGFPnls and *Kit*-MerCreMer mice were generated by standard gene targeting techniques. Homology arms upstream and downstream of the ATG start codon of the *Kit* gene in exon 1 were subcloned into a plasmid backbone containing Amp^r and a diphtheria toxin (DTA) cassette through recombineering. A cDNA encoding either Cre-IRES-eGFPnls (from Dr Andrew P. McMahon, UCLA) or MerCreMer, as well as an frt site-flanked neomycin selection cassette, were cloned in-frame with the *Kit* ATG start site. Embryonic stem (ES) cells were electroporated with linearized targeting vector. Targeted clones were identified by Southern blot and PCR. ES cell aggregation with 8-cell embryos was used to generate chimeric mice with the *Kit*-Cre-IRES-eGFPnls construct [31], while the *Kit*-MerCreMer mice were generated by blastocyst injection at the Howard Hughes Medical Institute (HHMI) gene-targeting core facility (by Dr Caiying Guo at HHMI, who also generated the *Kit*-MerCreMer targeting vector and targeted ES cells). Germline transmitting male chimeras were crossed with *Rosa26*-Flpe females (B6.129S4-*Gt(ROSA)26Sor*$^{tm1(FLP1)Dym}$/RainJ) to delete the neomycin cassette and verified offspring were further back-crossed to C57Bl/6J for 5 generations. Reporter mice FVB.Cg-*Gt(ROSA)26Sor*$^{tm1(CAG-lacZ,EGFP)Glh}$/J (previously modified by cross-breeding to B6(C3)-

Tg(Pgk1-FLPo)10Sykr/J) and B6.129(Cg)-*Gt(ROSA)26Sor*$^{tm4(ACTB-tdTomato,-EGFP)Luo}$/J were purchased from the Jackson Laboratories. *Kit* null mice were generated by breeding male $Kit^{+/Cre}$ with female $Kit^{+/MCM}$ × R-GFP mice, of which 1:8 embryos are predicted to be $Kit^{MCM/Cre}$ × R-GFP (nulls, with the reporter). Littermates that were $Kit^{+/Cre}$ × R-GFP were controls to show the full extent of $eGFP^{+}$ cardiomyocytes that are possible in the heart. Because *Kit* null mice were not identified at birth in multiple litters, we harvested mice from this cross at embryonic days 16.5 and 18.5, which identified viable *Kit* null embryos. PCR genotyping of *Kit*-Cre-IRES-eGFPnls used the following primers, (wt-Kit-Forward: 5'-CTGTAGCAGAGAGAGGAGCT-3' and Cre-Reverse: 5'-CTACACCAGAGACGGAAATCC-3'); *Kit*-MerCreMer (MerCreMer-Forward: 5'-CTGAACCGCCCATGATCTATT-3' and MerCreMer-Reverse: 5'-GTGGATGTGGTCCTTCTCTTC-3'); *Kit* (Forward: 5'-CTGTAGCAGAGAGAGGAGCT-3' and Reverse: 5'-ACAGAGGGTGCAGTCCTCTT-3'). Both sexes of mice were used for all xperiments.

Animal procedures

Tamoxifen citrate containing chow (Harlan laboratories) was used to activate the inducible MerCreMer protein, thereby inducing Cre recombinase activity. We used the standard 400 mg/kg chow for all experiments, except for labeling right after birth where we used 200 mg/kg. The duration of treatment is indicated within each experiment. Myocardial infarction (MI) was induced in mice via permanent surgical ligation of the left coronary artery [32]. Briefly, mice (both sexes) were anesthetized using isoflurane and a left lateral thoracotomy was performed. The left coronary artery was identified and ligated just below the left atrium. After closing the thoracotomy and expelling residual air, the mice were allowed to recover. Two-dimensional M-mode echocardiography was performed on mice anesthetized with 2% isoflurane, using a Hewlett Packard SONOS 5500 with a 15 MHz transducer. An average of 3 measurements was taken for each mouse. Group sizes were determined from past experience and based on statistical power calculations, and the number of mice is given in the figure or figure legends. Isoproterenol treatment was given via osmotic minipumps (Alzet) at 60 mg/kg/day (in 1 μM ascorbic acid) for 4 weeks. Mice were either sacrificed by CO_2 asphyxiation or by excision of the heart under deep isoflurane sedation. Isolated organs were fixed in 4% paraformaldehyde overnight, then processed for paraffin embedding for 3 hours, and immersed in Phosphate Buffered Saline (PBS) containing 30% sucrose overnight before embedding in OCT (Tissue-Tek) for cryo-sectioning.

Cell isolation

We isolated bone marrow cells by flushing femurs and tibiae with Hanks Balanced Salt Solution (HBSS). Briefly, bone marrow was flushed using a 25 gauge needle attached to a syringe containing 10 ml of ice cold HBSS supplemented with 2% fetal calf serum (FCS). Cells were spun at 400 g for 10 minutes at 4°C and pellets were re-suspended in 2% FCS/HBSS. After isolation, cells were kept on ice and further processed for flow cytometry or DNA extraction. Adult cardiomyocytes were isolated by removal of beating hearts from anesthetized mice and cannulated for retrograde perfusion with modified Tyrode solution (NaCl 120 mM, KCl 14.7 mM, KH_2PO_4 0.6 mM, Na_2HPO_4 0.6 mM, $MgSO_4$ 1.2 mM, HEPES 10 mM, $NaHCO_3$ 4.6 mM, Taurine 30 mM, Glucose 5.5 mM, butanedione

monoxime (BDM) 10 mM, pH7.40) supplemented with Liberase TH (Roche) [33]. After perfusion, hearts were disassociated into individual cardiomyocytes, calcium was gradually added back and cells were plated on laminin coated cover slips in modified Tyrode solution supplemented with 1 mg/ml 2,3-butanedione monoxime (BDM) and immediately counted for $eGFP^+$ cardiomyocytes. After counting, cells were imaged with a Nikon Eclipse TE300 inverted fluorescence microscope. Non-cardiomyocytes from the heart were isolated by retrograde perfusion as previously described [34]. Briefly, hearts were perfused with a digestion buffer (NaCl 126 mM, KCl 4.4 mM, $MgCl_2$ 5 mM, Na Pyruvate 5 mM, NaH_2PO_4 5 mM, Creatine 5 mM, HEPES 5 mM, Glucose 22 mM, Taurine 20 mM) containing 15 μM $CaCl_2$, collagenase type 2 (Worthington, 274 U/ml) and Protease XIV (Sigma-Aldrich, 0.57 U/ml). Cardiomyocytes were eliminated by 2 serial centrifugations at 10 g for 5 minutes at 4°C and the non-cardiomyocyte cell fraction was collected after a final centrifugation at 500 g for 10 minutes at 4°C.

Flow cytometry

Flow cytometry was performed on bone marrow and non-myocyte heart fractions using a BD FACSCanto II running FACSDiva software with the following configuration: 405nm laser for Alexa405, 633nm for APC and 488nm for GFP. Voltages were determined using single-stain and fluorescence minus one (FMO) controls. Analysis was performed using FlowJo vX. Hematopoietic lineage committed bone marrow cells were identified and negatively gated using a panel of mouse antibodies (CD3e, CD11b, CD45R/B220, Ly6G and Ly-6C, and TER-119; collectively Lin^-). $c\text{-}kit^+$ cells were identified by antibody labeling and then plotted for endogenous eGFP fluorescence. Alternatively, all bone marrow cells were labeled with c-kit antibody and then plotted for both c-kit positivity and endogenous eGFP fluorescence. Non-myocytes from the heart were first gated for eGFP fluorescence and plotted for CD45 or CD31 positivity. Summary of antibodies used is given in Supplementary Table 1

Multispectral-imaging flow cytometry

Quantitative real time c-kit and eGFP expression in bone marrow and non-cardiomyocyte cells from the hearts of $Kit^{+/Cre}$ × R-GFP mice was analyzed by ImageStreamX (Amnis, Seattle, WA), a multispectral flow cytometer combining standard microscopy with flow cytometry. We used the integrated software INSPIRE to run the ImageStreamX. For each experiment, cells were fixed and stained for c-kit antibody reactivity and suspended in 100 μl buffer (cold HBSS with 2% horse serum). Before running the samples, the ImageStreamX was calibrated using SpeedBeads (Amnis). Samples were acquired for unlabeled, single-color fluorescence controls, then the experimental samples. At least 10,000 experimental cells and 2,000 control cells were acquired for each sample. Images were analyzed using IDEAS image-analysis software (Amnis). Summary of antibodies used is given in Supplementary Table 1.

Immunohistochemistry

Please refer to Supplementary Table 1 for all antibody information and dilutions. For paraffin sections, isolated organs were fixed overnight in freshly diluted 4% paraformaldehyde, dehydrated and sectioned at 5 μm. Following citrate antigen retrieval

(BioGenex), the sections were blocked for one hour at room temperature in a blocking solution (PBS with 0.1% cold water fish skin gelatin, 1% bovine serum albumin, 0.1% Tween-20, and 0.05% NaN3), which was also used to dilute antibodies. For cryosections, isolated organs were fixed for 3 hours in freshly diluted 4% paraformaldehyde at 4 °C, rinsed with PBS and cryoprotected in 30% sucrose/PBS overnight before embedding in OCT (Tissue-Tek) and 10 μm cryosections were collected. Cryosections were blocked for 30 minutes at room temperature in a blocking solution (PBS with 5% goat serum, 2% bovine serum albumin, 0.1% Triton X-100), which was also used to dilute antibodies. Primary antibodies were incubated overnight at 4°C, secondary antibodies for 2 hours at room temperature, washes were performed in PBS. Cryosections were used to visualize native eGFP or tdTomato fluorescence from the different reporters or from the IRES-eGFP cassette built into the *Kit*-Cre allele. Images were acquired on an inverted Nikon A1R confocal microscope using NIS Elements AR 4.13. Some images were further processed in Photoshop or Image J to increase brightness/contrast of individual channels before generating a pseudo-colored overlay.

Genomic PCR and qPCR

Genomic DNA was prepared from mouse tissues or isolated mouse cardiomyocytes using the DNeasy Blood & Tissue Kit (Qiagen, 69504) per manufacturer's instructions. Briefly, cells or tissues were snap-frozen at time of harvest then lysed by incubation with proteinase K for 3 hours at 56 °C, followed by spin column purification and elution. Samples were treated with RNase A to remove contaminating RNA. PCR was performed to detect recombined and non-recombined *Rosa26* reporter alleles using primers 5'-tctgcttcactctccccatc (forward, against the CAG promoter/enhancer), 5'-gatcagcagcctctgttccaca (forward, against the PGKNeo cassette) and 5'-cgctgaacttgtggccgtttac (reverse, against eGFP). PCR conditions were 96°C for 2 minutes to separate strands, followed by 34 cycles of amplification (96°C for 30 s, 56°C for 30 s, 72°C for 30 s) and a 5 min elongation step at 72°C. PCR products were visualized on an ethidium bromide-stained agarose gel using a UV molecular imager (Bio-Rad). To quantify levels of recombined and non-recombined *Rosa26* alleles in genomic DNA, qPCR was performed using SYBR Green with the same primers used for PCR above (Applied Biosystems), and detection with a Bio-Rad CFx96 thermocycler. Simultaneous reactions using the primers above were performed to detect recombined versus non-recombined alleles.

Western Blots

Western blotting was performed essentially as described previously [35]. E16.5 embryos were homogenized in RIPA buffer containing protease inhibitor cocktail (Roche) with a dounce homogenizer. Forty micrograms of protein per sample were resolved on 10% SDS-PAGE gels, transferred onto PVDF membranes, immunoblotted with antibodies for c-kit (R&D Systems AF1356) and GAPDH (Fitzgerald 10R-G109a), and then incubated with the appropriate alkaline phosphate-linked secondary antibodies. The PVDF membranes were visualized by enhanced chemifluorescence (Amersham).

In vitro cardiomyocyte differentiation

The non-cardiomyocyte cell fraction was isolated from a 3 month-old $Kit^{+/Cre}$ × R-GFP mouse. Cells were plated at a density of 40,000 cells/well on gelatin coated 6-well tissue culture dishes in DMEM media containing 10% FCS, antibiotics and non-essential amino acids. After 2 days, the cells were washed and treated with 10 nM dexamethasone in DMEM containing 10% FCS to induce differentiation [6]. The media was refreshed every 3 days. After 1 week the cells were fixed with 4% paraformaldehyde and subjected to immunohistochemistry for vimentin, α actinin, troponin T, and GATA4 (antibodies listed in Supplementary Table 1). The cells were then imaged on an inverted Nikon A1R confocal microscope.

Statistics

For studies involving induction of MI, group sizes were determined based on previously observed post-operative mortality rates for this procedure. No experimental animals were excluded in any of the analyses. Blinding and randomization were not performed with the exception of the experiments in Supplemental Figure 1, which was done by two observers blinded to the sample identity. For flow cytometry experiments and direct counting of cardiomyocytes in histological sections or dissociated cardiomyocytes in dishes, two-group comparisons were performed using Student's two-tailed t-test, with $p<0.05$ considered statistically significant. All error bars throughout the figures are s.e.m. and all represented data are averages. When representative FACS plots or immunohistological images are shown, at least 3 independent samples were analyzed from separate mice.

Extended Data

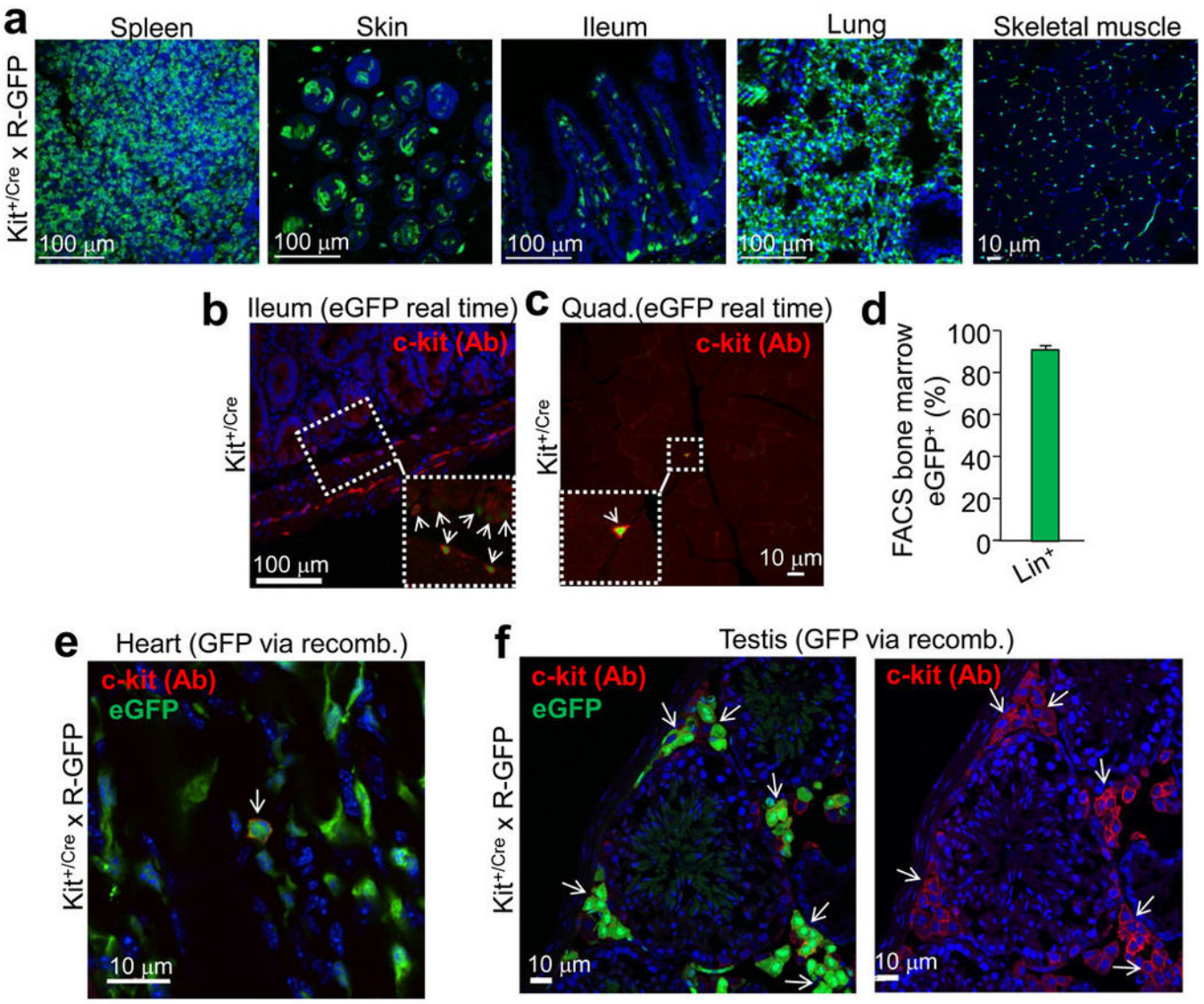

Extended Data Figure 1. Assessing the fidelity and specificity of the Kit-Cre knock-in allele

a, Histological sections from the indicated tissues of $Kit^{+/Cre}$ × R-GFP mice at 4 weeks of age. Blue is nuclei and green is eGFP. The data show eGFP expression in regions of each tissue that is often characteristic of endogenous c-kit protein expression. **b**, Immunohistochemistry for endogenous c-kit expression (red) in the mouse ileum at 4 weeks of age from $Kit^{+/Cre}$ mice that contain the IRES-eGFPnls cassette (but without the × R-GFP reporter allele) so that eGFP expression can be monitored in real time. The inset box and arrows show the co-staining with c-kit antibody and eGFP. **c**, Immunohistochemistry for endogenous c-kit expression (red) in quadriceps muscle of $Kit^{+/Cre}$ mice at 4 weeks of age versus nuclear eGFP (green) from the $Kit^{+/Cre}$ allele. While lineage tracing in $Kit^{+/Cre}$ × R-GFP mice, which is cumulative, showed abundant endothelial cells throughout the skeletal muscle (**a**), instantaneous c-kit expressing cells are rare in skeletal muscle, and when

identified, are always mononuclear (inset box). **d**, FACS quantitation of bone marrow from Kit$^{+/Cre}$ × R-GFP mice at 4 weeks of age sorted for eGFP expression, of which 94% are positive for the "lineage" cocktail of differentiation-specific antibodies (n=3 mice). Hence the *Kit*-Cre allele is properly expressed in bone marrow and traces lineages that arise from c-kit^{+} progenitors. **e**, Immunohistochemistry in the hearts of Kit$^{+/Cre}$ × R-GFP mice for endogenous c-kit expression (red) versus all the cells that underwent recombination throughout development and the first 4 weeks of life, shown in green. While cells that are actively expressing c-kit protein are very rare in the heart (≈5 per heart section), the arrow shows such a cell that is also eGFP^{+} for recombination. All of the currently c-kit expressing cells identified in the heart were eGFP^{+}, further verifying the fidelity of the *Kit*-Cre allele. **f**, Same experiment as in **e** except the testis was examined because of the characteristic pattern of Leydig cells that are known to be actively c-kit expressing cells. The data show that greater than 80% of the currently c-kit antibody reactive Leydig cells (red outline, better observed in the right panel) are also eGFP^{+} (arrows show clusters of these cells).

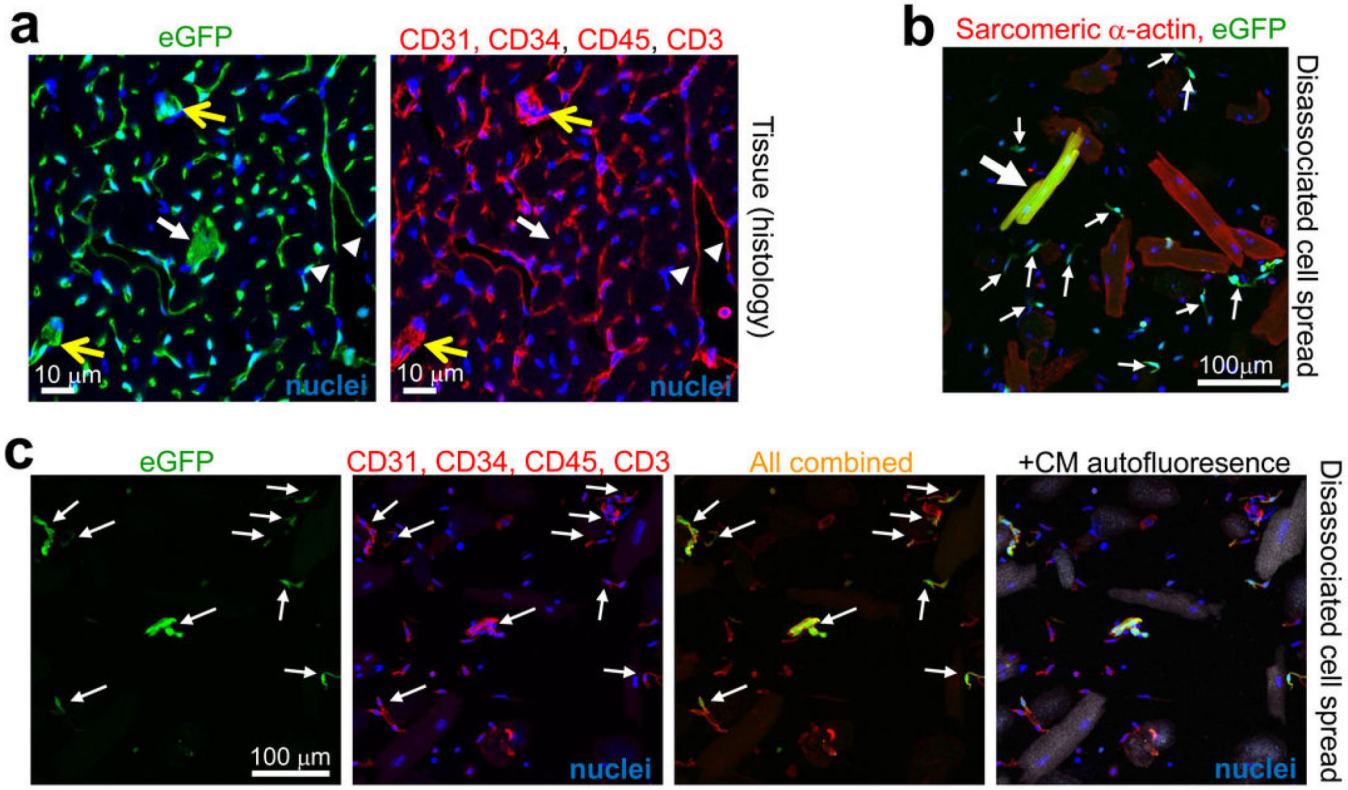

Extended Data Figure 2. Identification of non-myocytes from the hearts of Kit$^{+/Cre}$ × R-GFP mice

Kit$^{+/Cre}$ × R-GFP mice were harvested at 6 weeks of age (constitutive lineage labeling the entire time), although MI was performed at week 4 to induce greater vascular remodeling and potentially more c-kit lineage recruitment over the next 2 weeks. **a,** Hearts were then collected at week 6 and subjected to immunohistochemistry with a pool of antibodies for CD31, CD34, CD45 and CD3 in red, while the green channel was for eGFP expression from the recombined R-GFP reporter allele due to *Kit*-Cre lineage expression. The white

arrowheads show endothelial cells that are not contiguous with the underlying network, although most of the endothelial cells are from the c-kit lineage when the red and green channels are compared. The white arrow shows a cardiomyocyte that lacks red staining, while the yellow arrows show 2 areas with relatively large cells that are eGFP^{+} and could be mistaken for a cardiomyocyte, although they are also positive for the non-myocyte marker panel of antibodies. **b, c,** Spread of cells isolated from hearts of 8 week-old Kit$^{+/Cre}$ × R-GFP mice at baseline that were subjected to immunocytochemistry for the indicated markers. The large white arrow in panel **b** shows an eGFP^{+} (green) cardiomyocyte that also co-stains with sarcomeric α-actin (red). The smaller arrows show eGFP^{+} non-myocytes, which in panel **c**, were subject to staining with a cocktail of antibodies again for CD31, CD34, CD45 and CD3 (all in red). This analysis identifies nearly all of the non-myocytes in these cell spreads. The very last image in panel **c** shows a fourth channel with higher gain so that the underlying cardiomyocytes (CMs) autofluoresce (in white) to show the mixed nature of the spread cells. Nuclei were stained blue with DAPI in the indicated panels.

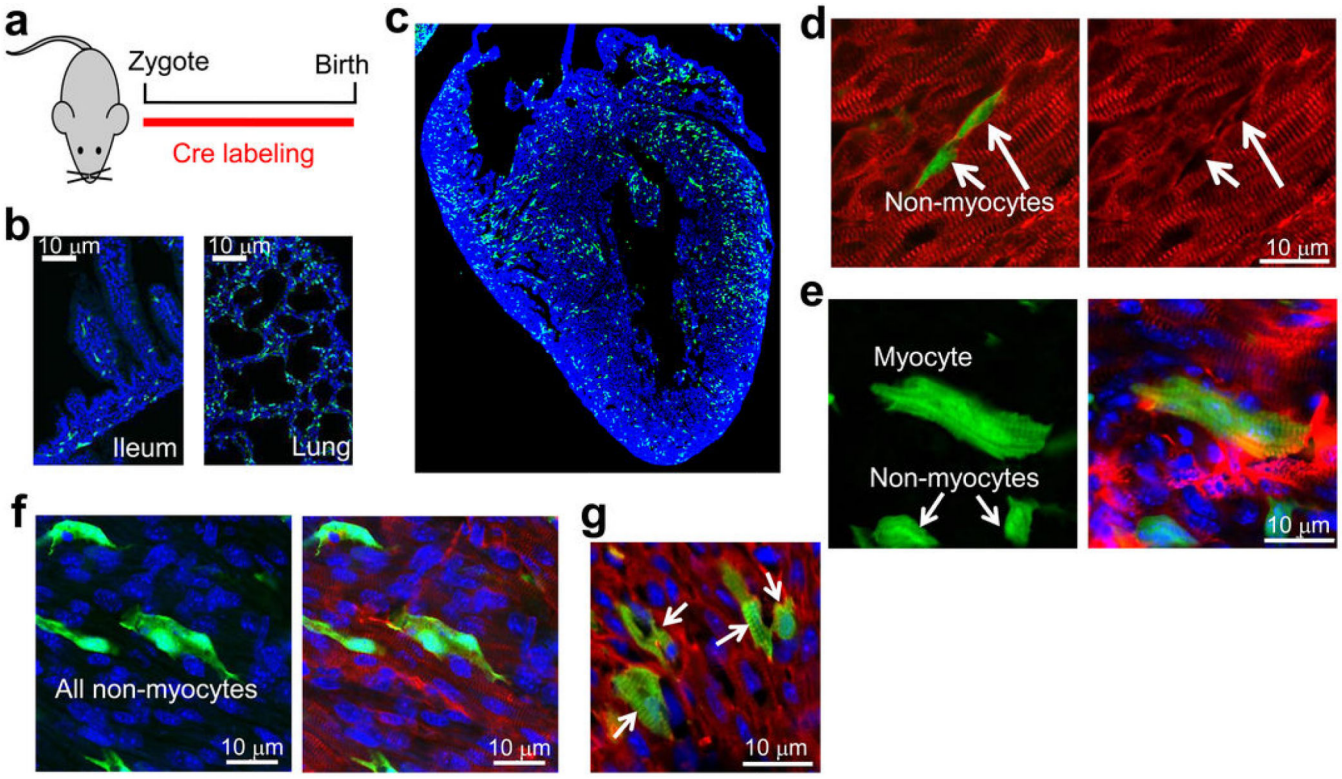

Extended Data Figure 3. Analysis of c-kit lineage labeling in the heart at P0 (birth)

a, Diagram of the timing whereby newborn Kit$^{+/Cre}$ × R-GFP mice were analyzed for all subsequent experiments in this figure. **b,** Histological sections for eGFP fluorescence (green) from the ileum and lung at P0 showing the characteristic c-kit labeling pattern as observed at other time points or in other studies when antibodies were employed. Blue shows nuclei **c,** Histological section for eGFP fluorescence (green) from the heart at P0. Blue shows nuclei and magnification was 40X. **d,** Immunohistochemical tissue section from the P0 heart of Kit$^{+/Cre}$ × R-GFP mice stained with sarcomeric α-actin (red) to show all underlying cardiomyocytes (right panel) or with eGFP expression in green (left panel) as

being c-kit derived. The green cells noted by the arrows are non-myocytes that do not express sarcomeric α-actin. **e,** eGFP expression alone (left) or eGFP with co-staining for cardiomyocytes in red (sarcomeric α-actin) from heart sections at P0 of $Kit^{+/Cre}$ × R-GFP mice. Blue staining depicts nuclei. The cardiomyocyte that is shown has clear striations in the eGFP staining pattern, while the 2 non-myocytes do not show striated eGFP and also lack sarcomeric α-actin staining. **f,** eGFP expression alone in green (left) with nuclei in blue or eGFP with sarcomeric α-actin co-staining (red) from heart sections at P0 of $Kit^{+/Cre}$ × R-GFP mice. All $eGFP^{+}$ cells shown lack striations and are non-myocytes although the 2 cells in the center sit directly on top of cardiomyocytes and could be easily mis-interpreted. Great care is needed in scoring myocytes in the P0 heart because they are small and often the same size as $eGFP^{+}$ non-myocytes. **g,** eGFP expression (green) with nuclei in blue and cardiomyocytes identified in red with sarcomeric α-actin antibody from heart histological sections at P0 of $Kit^{+/Cre}$ × R-GFP mice. Here the data show c-kit lineage derived cardiomyocytes that appear in a loose cluster (arrows), presumably from a clonal expansion event earlier in development.

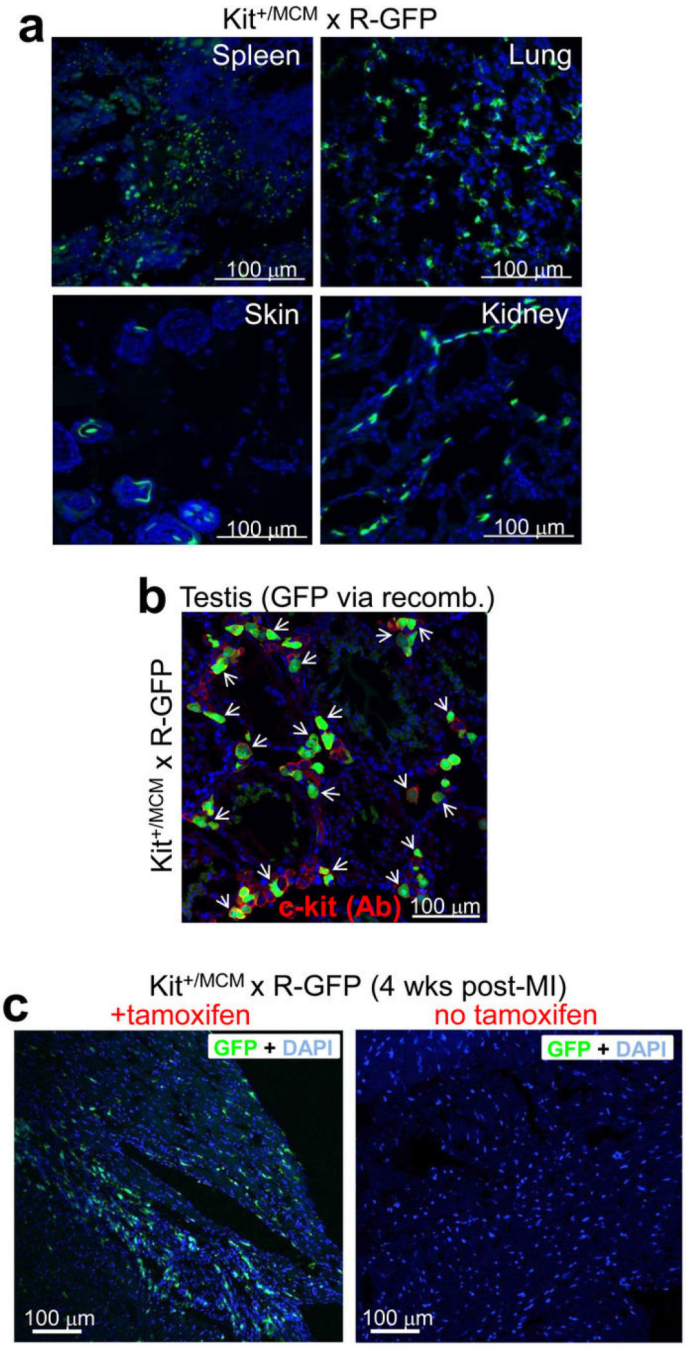

Extended Data Figure 4. Additional examination of the Kit-MerCreMer knock-in allele and its potential leakiness in the absence of tamoxifen

a, Histological analysis of eGFP fluorescent cells from the indicated tissues at day 28 from $Kit^{+/MCM}$ × R-GFP mice that were given tamoxifen from 2 to 28 days. Nuclei are shown in blue and green shows eGFP fluorescing cells in the expected patterns for known regions of c-kit protein expression, such as the distinct pattern of melanocytes in the skin and widespread expression in the spleen and lungs. **b**, Immunohistochemistry in the testis of $Kit^{+/MCM}$ × R-GFP mice for endogenous c-kit expression (red) versus cells that underwent

recombination when tamoxifen was given by intraperitoneal injection (2 mg) for 5 consecutive days (green). The data show that most of the currently c-kit protein expressing cells in testis (only Leydig cells react, red surface staining) are also eGFP^{+} (intracellular), indicating that recombination only occurs in c-kit expressing cells, and the majority of them. **c**, Histological sections through the heart showing that the *Kit*-MerCreMer allele does not leak at baseline or after MI injury (n=3 mice per treatment). Kit$^{+/MCM}$ × R-GFP mice were placed on tamoxifen-laden food or vehicle food beginning at 4 weeks of age and then subjected to MI injury 4 weeks later, followed by harvesting 4 weeks after that. In the presence of tamoxifen histological sections through the MI border zone of the heart show wide-spread eGFP^{+} cells (green) from the c-kit lineage (left panel), while in the absence of tamoxifen no eGFP^{+} cells are observed (right panel), hence the *Kit*-MerCreMer allele does not leak.

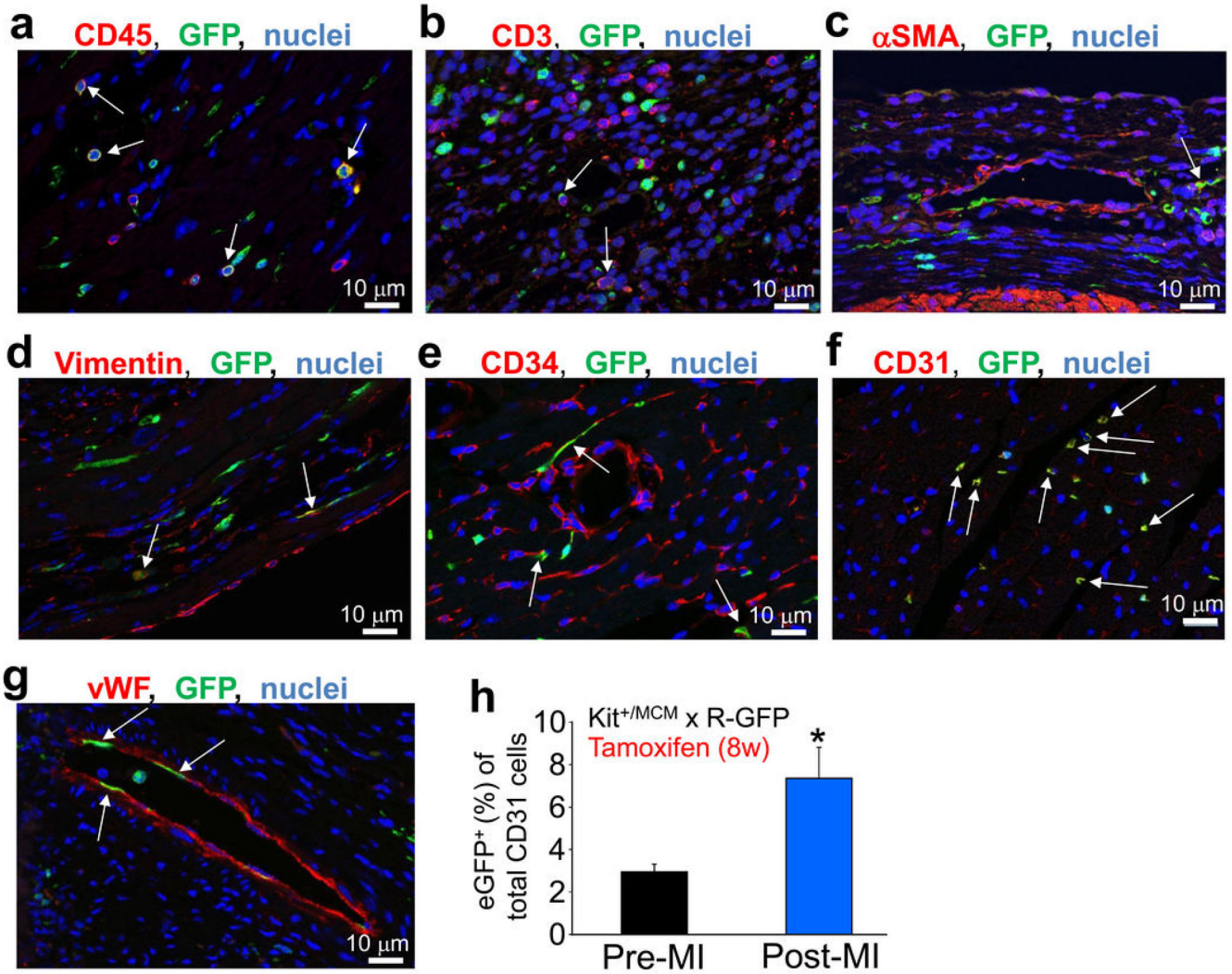

Extended Data Figure 5. Analysis of eGFP^{+} non-myocytes in the hearts of Kit$^{+/MCM}$ × R-GFP mice at baseline or after MI injury

a–g,Tamoxifen was given to Kit$^{+/MCM}$ × R-GFP mice for 1 day – 6 months of age (**a,e,f**) or in mice given tamoxifen and MI injury (**b,c,d,g**), followed by harvesting the hearts for immunohistochemistry with antibodies for GFP (green), or the indicated antibodies in red; (**a**) CD45, (**b**) CD3, (**c**) smooth muscle α-actin (αSMA), (**d**) vimentin, (**e**) CD34, (**f**) CD31, (**g**) von Willebrand factor (vWF). Nuclei are shown in blue. The white arrows show cells with coincident green and red reactivity for each of the markers, although sometimes the red marker is membrane localized while the green (eGFP) is always cytoplasmic. The most overlapping activity with GFP expression was observed for CD31 (endothelial cells), then CD34, followed by CD45 (hematopoietic cells). **h**, Quantitation from FACS plots of total CD31 cells (antibody) in the heart that are also eGFP^{+} from Kit$^{+/MCM}$ × R-GFP mice (Pre-MI, n=3) after 8 weeks of tamoxifen in early adulthood at either baseline or 4 weeks after MI injury (Post-MI, n=3). The data show about a doubling in the number of CD31 cells that are eGFP^{+} after MI (*P<0.05 vs pre-MI).

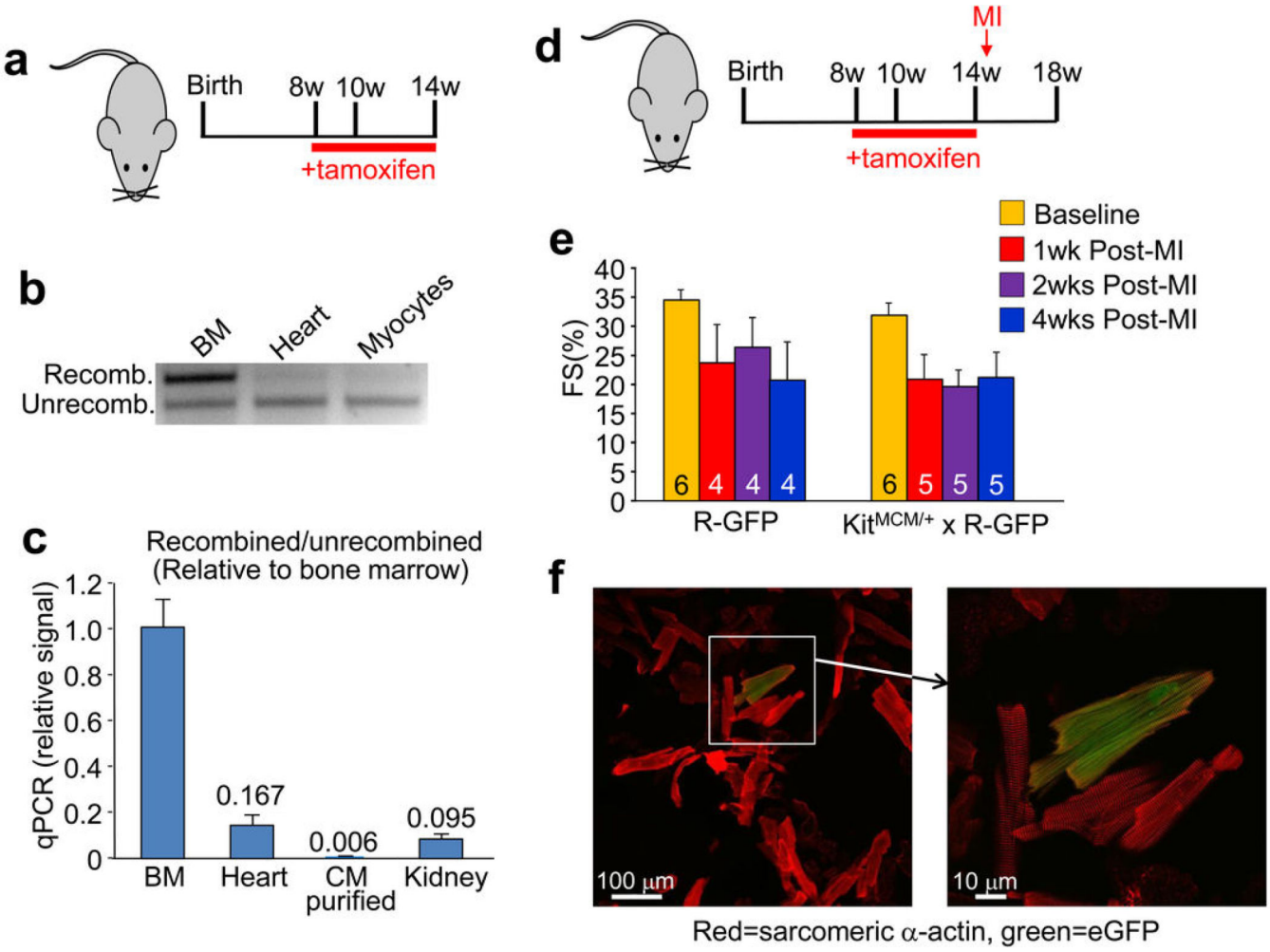

Extended Data Figure 6. Quantitation of Cre activity and DNA recombination in the hearts of Kit$^{+/MCM}$ × R-GFP mice

a, Time line for tamoxifen administration in Kit$^{+/MCM}$ × R-GFP mice. **b,** PCR from DNA generated from the bone marrow (BM), whole heart or semi-purified cardiomyocytes after 6

weeks of tamoxifen treatment in $Kit^{+/MCM}$ × R-GFP mice (n=2). Bone marrow shows most of the DNA as having been recombined by Cre, while whole heart is just barely discernable, and purified cardiomyocytes show essentially no recombination given the sensitivity constraints of this assay. **c,** qPCR was also run to more sensitively detect and quantify the extent of recombination, which was set relative to the recombination in bone marrow. Semi-purified cardiomyocytes (CM) showed very low rates. Averaged data are shown and error bars are s.e.m. of duplicate technical replicates from *n*=3 $Kit^{+/MCM}$ × R-GFP mice. **d,** Schematic of the tamoxifen time course and timing of myocardial infarction (MI) in $Kit^{+/MCM}$ × R-GFP mice. **e,** Echocardiography measured cardiac fractional shortening (FS %) was assessed in the mice after MI, which shows a reduction in cardiac ventricular performance at 1, 2 and 4 weeks after injury. The number of mice analyzed is shown in the bars. Error bars represent the s.e.m. Both the control and experimental groups showed an equivalent reduction in cardiac function post-MI. **f,** Images of dissociated cardiomyocytes from hearts of $Kit^{+/MCM}$ × R-GFP mice 4 weeks after MI, which were fixed and stained for sarcomeric α-actin antibody (red) and eGFP (green) at 2 different magnifications. One $eGFP^{+}$ cardiomyocyte is shown with sarcomeric patterning of the eGFP fluorescence.

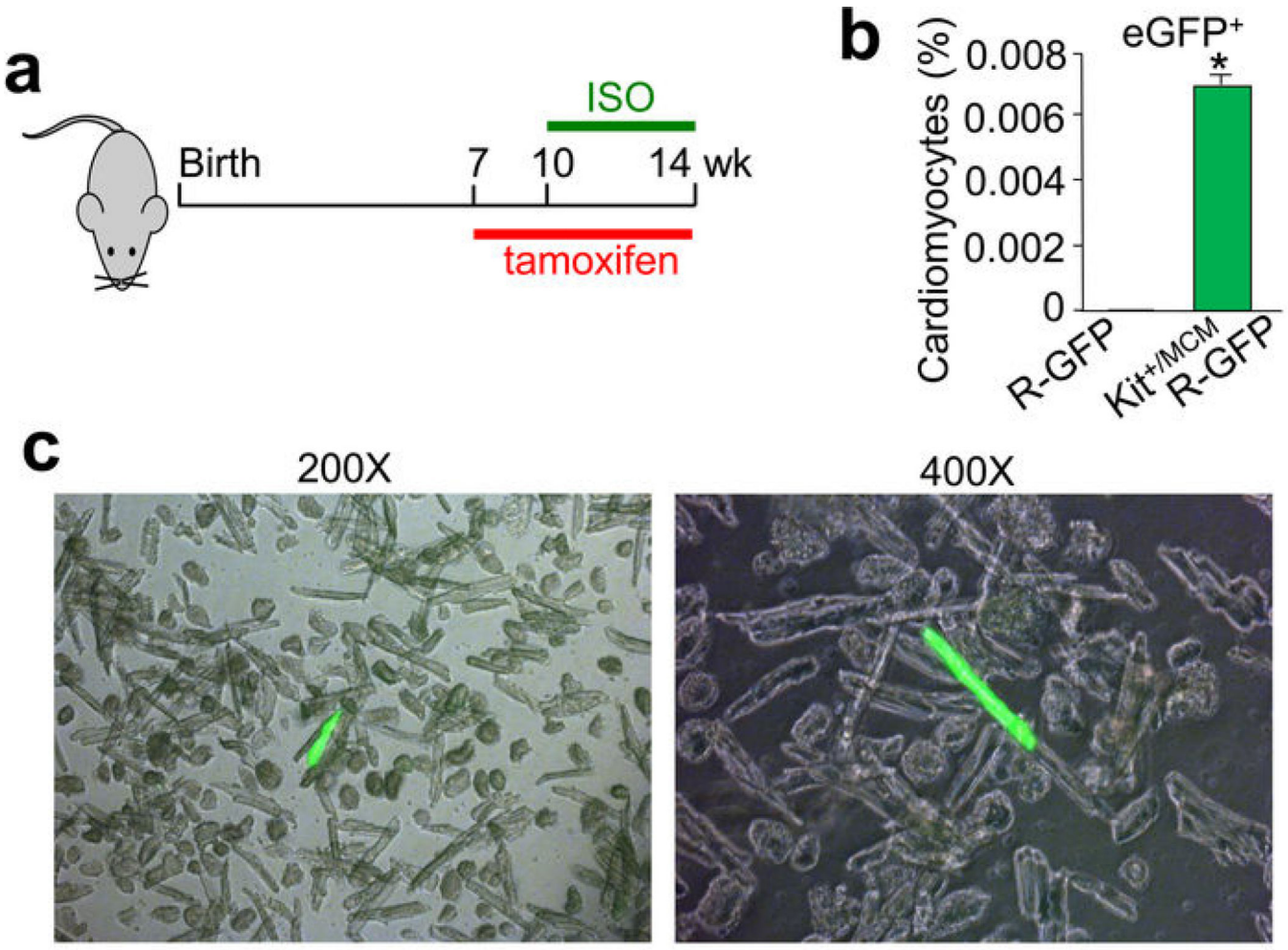

Extended Data Figure 7. Analysis of eGFP^{+} myocytes in the hearts of Kit$^{+/MCM}$ × R-GFP mice after isoproterenol infusion-induced injury

a, Schematic diagram showing tamoxifen treatment of Kit$^{+/MCM}$ × R-GFP mice between 7 and 14 weeks of age with isoproterenol (ISO) infusion occurring between weeks 10–14. **b, c,** Quantitation and imaging of disassociated cardiomyocytes (separate images shown at 2 different magnifications) from the hearts of ISO injured Kit$^{+/MCM}$ × R-GFP mice, which showed rare but definitive cardiomyocyte labeling. *P<0.05 vs R-GFP, 31 eGFP^{+} cells of 395,302 counted from 2 hearts.

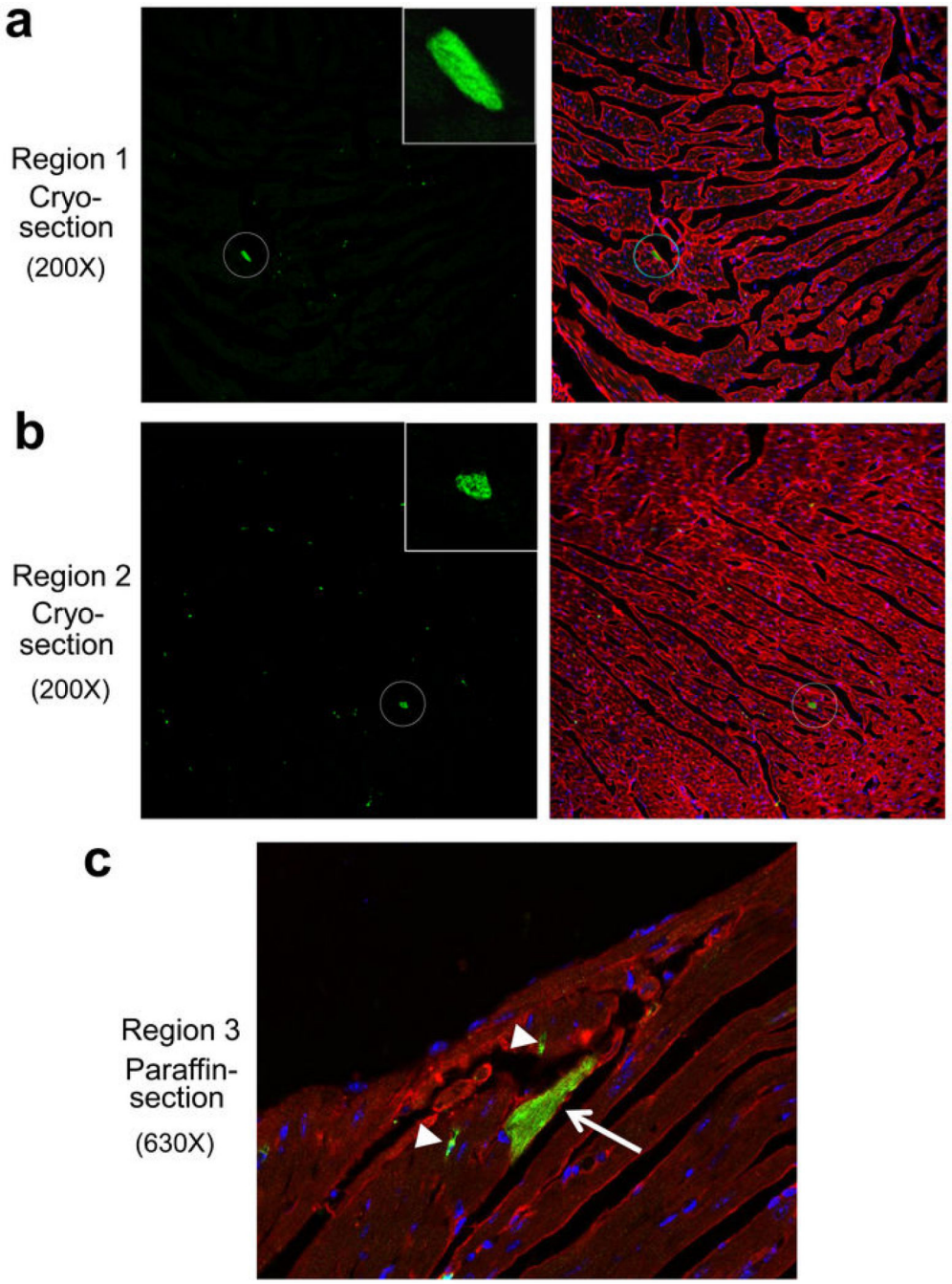

Extended Data Figure 8. Verifying the extent of eGFP$^+$ cardiomyocytes by an independent laboratory from blinded histological heart samples

Unprocessed cryosections and paraffin sections from the hearts of Kit$^{+/MCM}$ × R-GFP mice after 8 weeks of tamoxifen were blinded and sent to the Marbán laboratory along with negative control sections from hearts that should not have staining. **a, b,** Two separate images from cryo-preserved blocks are shown at 200x magnification in which the cryo-section was processed for eGFP fluorescence (green) and α-actinin antibody (red) to show cardiomyocytes. The data show 2 regions where a single eGFP$^+$ myocyte is visible in a region with several hundred GFP-negative cardiomyocytes. The single eGFP$^+$ cardiomyocyte is circled and the inset box shows a higher magnification. Sections were also stained for nuclei (blue). In general, approximately 1–2 definitive eGFP$^+$ cardiomyocytes were identified per entire heart section in the Marbán laboratory, a result that is consistent with the approximate numbers of kit lineage-labeled cardiomyocytes observed by us. **c,** Image taken at 630x magnification from a paraffin embedded and processed histological section in which both an eGFP antibody (green) and α-actinin antibody (red) was used. Nuclei are shown in blue. The arrow shows a single eGFP$^+$ expressing cardiomyocyte and the arrowheads show eGFP$^+$ non-myocytes.

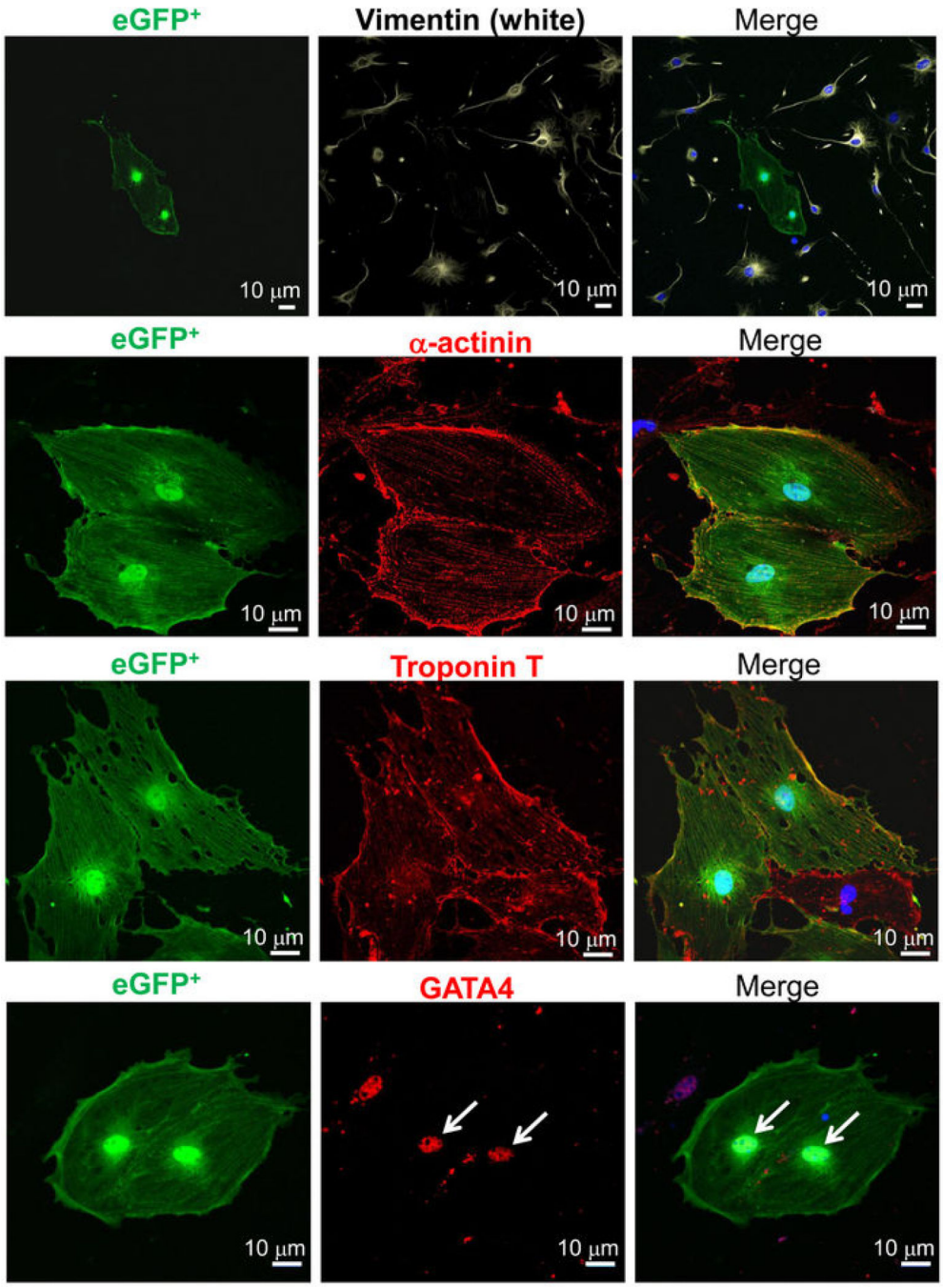

Extended Data Figure 9. Assessing cardiomyocyte differentiation markers from total non-myocytes in the heart

Adult cardiac interstitial cells isolated from a $Kit^{+/Cre}$ × R-GFP mouse were treated with dexamethasone for 1 week. Cells were then fixed and subjected to immunocytochemistry for the indicated antibodies. c-kit lineage derived cells were green ($eGFP^{+}$) and showed fluorescence in the cytosol and nucleus. The data show eGFP cells that express markers of differentiated cardiomyocytes such as α-actinin, troponin T, and the transcription factor GATA4 (all in red) but not the fibroblast marker vimentin (white), nuclei were stained blue (right panels). These results indicate that $eGFP^{+}$ *Kit*-Cre expressing cells can generate pre-

differentiated cardiomyocytes as well as non-eGFP interstitial cells; hence the cells identified by the *Kit*-Cre (knock-in) reporter strategy are representative of how endogenous c-kit$^+$ expressing cells truly function.

Supplementary Material

Refer to Web version on PubMed Central for supplementary material.

Acknowledgements

This work was supported by grants from the NIH (to J.H.v.B., E.M., and J.D.M.). J.D.M. is an investigator of the Howard Hughes Medical Institute.

References

1. Laflamme MA, Murry CE. Heart regeneration. Nature. 2011; 473:326–335. [PubMed: 21593865]
2. Orlic D, et al. Bone marrow cells regenerate infarcted myocardium. Nature. 2001; 410:701–705. [PubMed: 11287958]
3. Balsam LB, et al. Haematopoietic stem cells adopt mature haematopoietic fates in ischaemic myocardium. Nature. 2004; 428:668–673. [PubMed: 15034594]
4. Murry CE, et al. Haematopoietic stem cells do not transdifferentiate into cardiac myocytes in myocardial infarcts. Nature. 2004; 428:664–668. [PubMed: 15034593]
5. Anversa P, Kajstura J, Rota M, Leri A. Regenerating new heart with stem cells. J Clin Invest. 2013; 123:62–70. [PubMed: 23281411]
6. Beltrami AP, et al. Adult cardiac stem cells are multipotent and support myocardial regeneration. Cell. 2003; 114:763–776. [PubMed: 14505575]
7. Hosoda T, et al. Clonality of mouse and human cardiomyogenesis in vivo. Proc Natl Acad Sci U S A. 2009; 106:17169–17174. [PubMed: 19805158]
8. Ellison GM, et al. Adult c-kit(pos) cardiac stem cells are necessary and sufficient for functional cardiac regeneration and repair. Cell. 2013; 154:827–842. [PubMed: 23953114]
9. Jesty SA, et al. c-kit+ precursors support postinfarction myogenesis in the neonatal, but not adult, heart. Proc Natl Acad Sci U S A. 2012; 109:13380–13385. [PubMed: 22847442]
10. Zaruba MM, Soonpaa M, Reuter S, Field LJ. Cardiomyogenic potential of C-kit(+)-expressing cells derived from neonatal and adult mouse hearts. Circulation. 2010; 121:1992–2000. [PubMed: 20421520]
11. Ro S, et al. A model to study the phenotypic changes of interstitial cells of Cajal in gastrointestinal diseases. Gastroenterology. 2010; 138:1068–1078. e1061–e1062. [PubMed: 19917283]
12. Okura M, Maeda H, Nishikawa S, Mizoguchi M. Effects of monoclonal anti-c-kit antibody (ACK2) on melanocytes in newborn mice. J Invest Dermatol. 1995; 105:322–328. [PubMed: 7545201]
13. Sandlow JI, Feng HL, Cohen MB, Sandra A. Expression of c-KIT and its ligand, stem cell factor, in normal and subfertile human testicular tissue. J Androl. 1996; 17:403–408. [PubMed: 8889703]
14. Alvarez-Dolado M, et al. Fusion of bone-marrow-derived cells with Purkinje neurons, cardiomyocytes and hepatocytes. Nature. 2003; 425:968–973. [PubMed: 14555960]
15. Matsuura K, et al. Cardiomyocytes fuse with surrounding noncardiomyocytes and reenter the cell cycle. J Cell Biol. 2004; 167:351–363. [PubMed: 15492039]
16. Nygren JM, et al. Bone marrow-derived hematopoietic cells generate cardiomyocytes at a low frequency through cell fusion, but not transdifferentiation. Nat Med. 2004; 10:494–501. [PubMed: 15107841]
17. Oh H, et al. Cardiac progenitor cells from adult myocardium: homing, differentiation, and fusion after infarction. Proc Natl Acad Sci U S A. 2003; 100:12313–12318. [PubMed: 14530411]

18. Terada N, et al. Bone marrow cells adopt the phenotype of other cells by spontaneous cell fusion. Nature. 2002; 416:542–545. [PubMed: 11932747]
19. Peters EM, Tobin DJ, Botchkareva N, Maurer M, Paus R. Migration of melanoblasts into the developing murine hair follicle is accompanied by transient c-Kit expression. J Histochem Cytochem. 2002; 50:751–766. [PubMed: 12019292]
20. Waskow C, Paul S, Haller C, Gassmann M, Rodewald HR. Viable c-Kit(W/W) mutants reveal pivotal role for c-kit in the maintenance of lymphopoiesis. Immunity. 2002; 17:277–288. [PubMed: 12354381]
21. Mauduit C, Hamamah S, Benahmed M. Stem cell factor/c-kit system in spermatogenesis. Hum Reprod Update. 1999; 5:535–545. [PubMed: 10582791]
22. Ro S, et al. A model to study the phenotypic changes of interstitial cells of Cajal in gastrointestinal diseases. Gastroenterology. 2010; 138:1068–1078. [PubMed: 19917283]
23. Ye L, et al. Aging Kit mutant mice develop cardiomyopathy. PLoS One. 2012; 7:e33407. [PubMed: 22428044]
24. Bolli R, et al. Cardiac stem cells in patients with ischaemic cardiomyopathy (SCIPIO): initial results of a randomised phase 1 trial. Lancet. 2011; 378:1847–1857. [PubMed: 22088800]
25. Soonpaa MH, Field LJ. Assessment of cardiomyocyte DNA synthesis in normal and injured adult mouse hearts. Am J Physiol. 1997; 272:H220–H226. [PubMed: 9038941]
26. Angert D, et al. Repair of the injured adult heart involves new myocytes potentially derived from resident cardiac stem cells. Circ Res. 2011; 108:1226–1237. [PubMed: 21454756]
27. Hsieh PC, et al. Evidence from a genetic fate-mapping study that stem cells refresh adult mammalian cardiomyocytes after injury. Nat Med. 2007; 13:970–974. [PubMed: 17660827]
28. Bergmann O, et al. Evidence for cardiomyocyte renewal in humans. Science. 2009; 324:98–102. [PubMed: 19342590]
29. Senyo SE, et al. Mammalian heart renewal by pre-existing cardiomyocytes. Nature. 2013; 493:433–436. [PubMed: 23222518]
30. Kajstura J, et al. Cardiomyogenesis in the aging and failing human heart. Circulation. 2012; 126:1869–1881. [PubMed: 22955965]

Additional references

31. Nagy, A.; Rossant, J. Gene Targeting:A Practical Approach. 2 edition. Joyner, Alexandra L., editor. Oxford University Press, USA; 2000.
32. Liu Q, Sargent MA, York AJ, Molkentin JD. ASK1 regulates cardiomyocyte death but not hypertrophy in transgenic mice. Circ Res. 2009; 105:1110–1117. [PubMed: 19815822]
33. Nakayama H, et al. alpha1G-dependent T-type Ca2+ current antagonizes cardiac hypertrophy through a NOS3-dependent mechanism in mice. J Clin Invest. 2009; 119:3787–3796. [PubMed: 19920353]
34. Hosoda T, et al. Clonality of mouse and human cardiomyogenesis in vivo. Proc Natl Acad Sci U S A. 2009; 106:17169–17174. [PubMed: 19805158]
35. Karch J, et al. Bax and Bak function as the outer membrane component of the mitochondrial permeability pore in regulating necrotic cell death in mice. Elife. 2013; 2:e00772. [PubMed: 23991283]

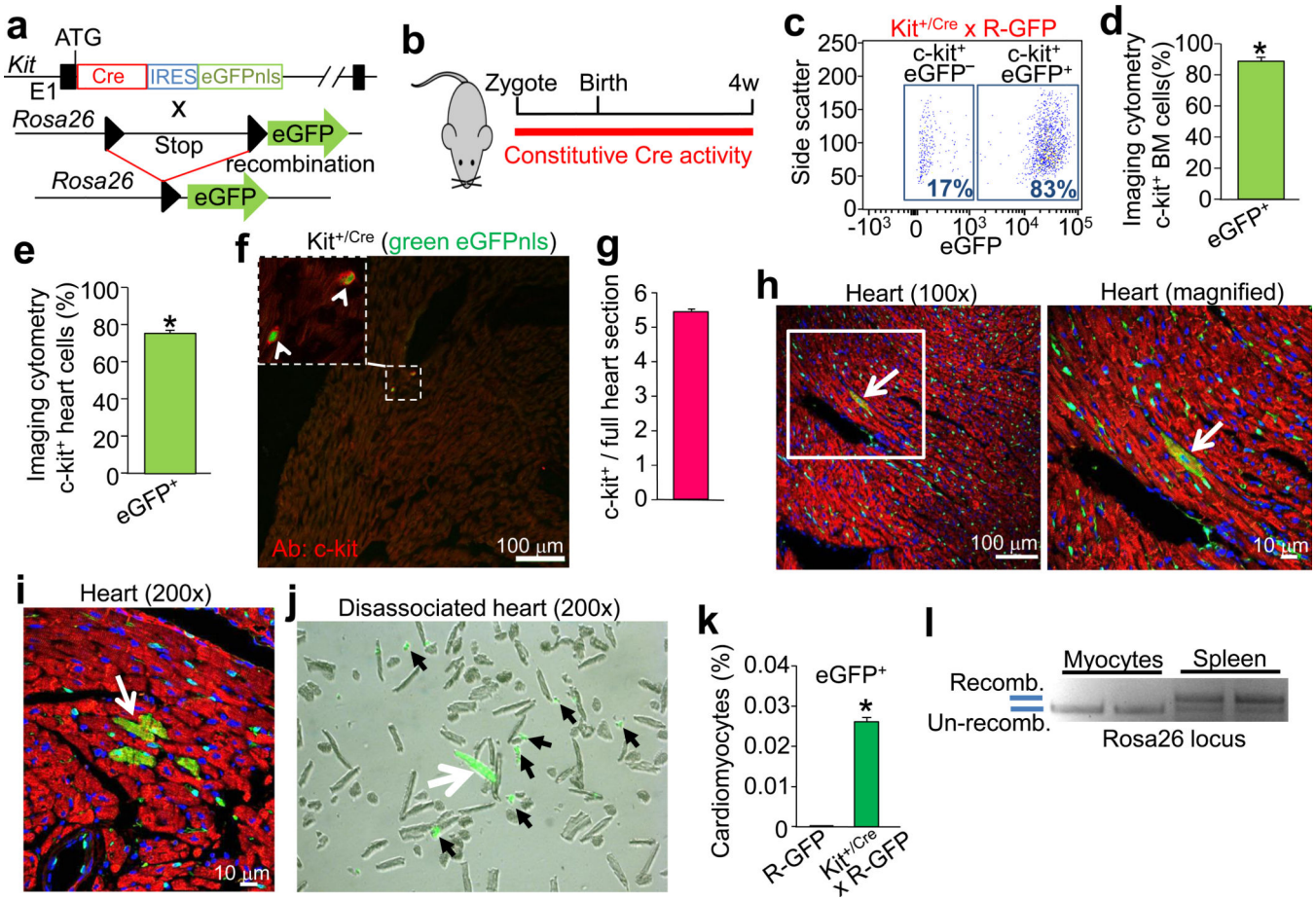

Figure 1. *Kit*-Cre lineage tracing

a, The *Kit* locus was targeted in mice to express Cre recombinase and eGFP with a nuclear localization sequence (eGFPnls) from an internal ribosome entry site (IRES). These mice were crossed with *Rosa26* reporter mice (R-GFP) for lineage tracing. **b**, Diagram of mice used for all experimentation in this figure. **c,** Representative flow cytometry (FACS) plot of bone marrow from $Kit^{+/Cre}$ × R-GFP mice gated for c-kit antibody, then eGFP fluorescence to reflect recombination of the R-GFP locus (representative of n=6 total). **d,** Direct imaging cytometry analysis of eGFP expression in bone marrow (n=3, *P<0.05 vs R-GFP). **e,** same quantitative imaging cytometry analysis as in **d** except the non-myocytes were isolated from hearts of $Kit^{+/Cre}$ × R-GFP mice (n=3 hearts, *P<0.05 vs R-GFP). **f**, Immunohistochemistry to show current expression from the *Kit*-Cre allele (green, eGFPnls) versus endogenous c-kit protein detected by antibody (red). The inset box shows 2 mononuclear c-kit expressing cells. **g**, Quantitation of average number of $c\text{-}kit^{+}$ cells per longitudinal heart section (n=4 hearts) **h,** Representative histological section at 2 magnifications (white box) of a $Kit^{+/Cre}$ × R-GFP mouse heart with desmin antibody in red, eGFP antibody in green, and nuclei in blue. The arrow shows an $eGFP^{+}$ cardiomyocyte. **i,** Immunohistological image showing a rare area of cardiomyocyte clonal expansion (arrow). **j,** Image of cells disassociated from the hearts of $Kit^{+/Cre}$ × R-GFP mice. White arrow shows a rare eGFP fluorescing cardiomyocyte, while the black arrowheads show eGFP fluorescent non-myocytes. **k**, Quantitation of $eGFP^{+}$ fluorescent cardiomyocytes (81 from 303,264 total cardiomyocytes,

3 hearts,*P<0.05 vs R-GFP). **l,** DNA electrophoresis after PCR showing Cre-mediated *Rosa26* locus recombination in semi-purified cardiomyocytes and spleen (n=2 each). All error bars represent s.e.m.

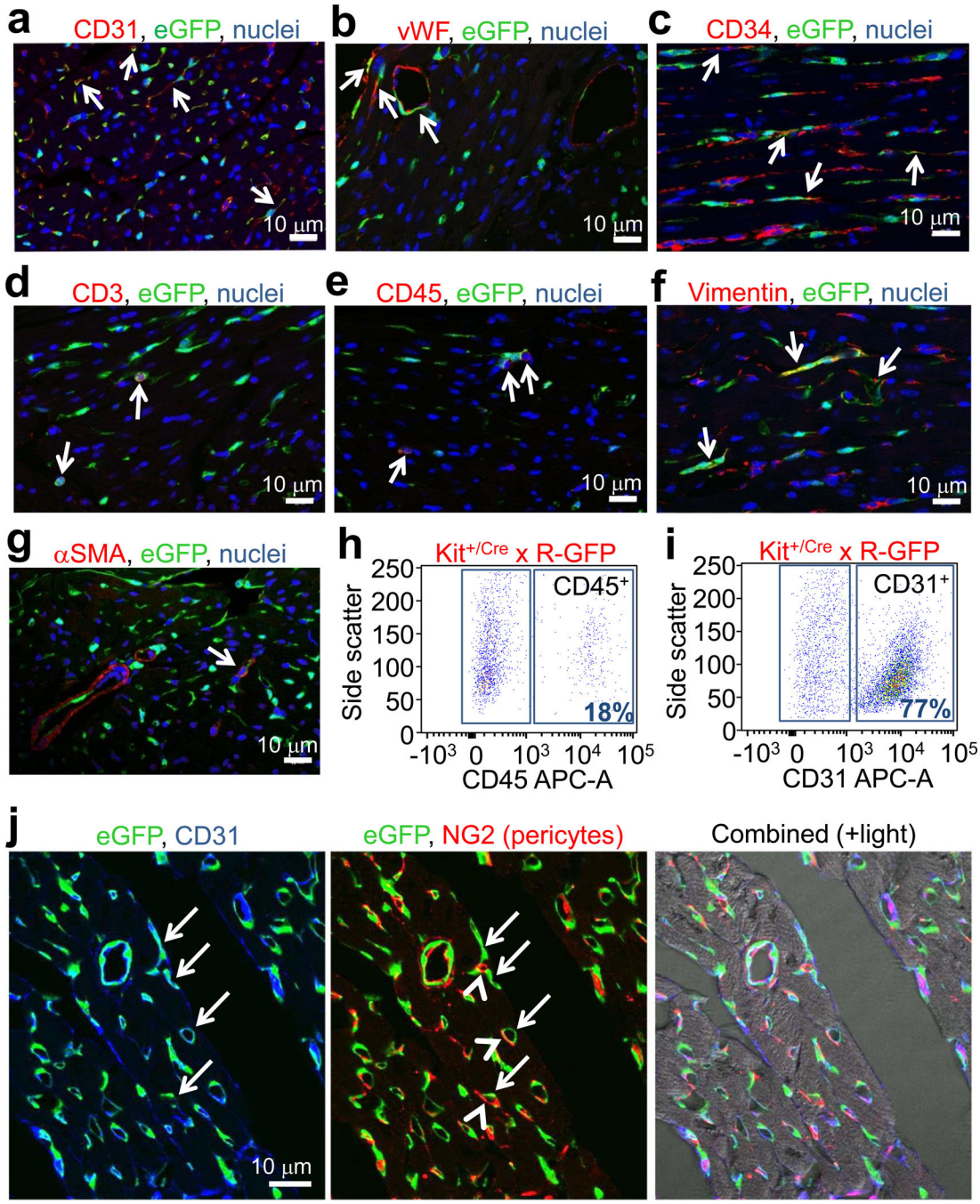

Figure 2.

Analysis of cardiac cells from Kit$^{+/Cre}$ × R-GFP mice. **a, b, c, d, e, f, g,** Immunofluorescent images of heart histological sections from Kit$^{+/Cre}$ × R-GFP mice at 4 weeks of age stained with eGFP antibody (green), nuclei in blue and either CD31, von Willebrand factor (vWF), CD34, CD3, CD45, vimentin or smooth muscle α-actin (αSMA) in red. Arrows show cells with overlap in staining. **h, i,** FACS plot showing lineage markers of heart isolated c-kit derived eGFP^{+} cells for CD45 (**h**) and CD31 (**i**) (representative of n=6 for CD45 at 4 weeks of age, and n=3 for CD31 at 12 weeks of age). **j**, Immunofluorescent image from heart

histological section of a $Kit^{+/Cre}$ × R-GFP mouse at 4 weeks for eGFP fluorescence (green), CD31 antibody staining (blue) and NG2 antibody staining (red). Right panel shows composite with transmitted light.

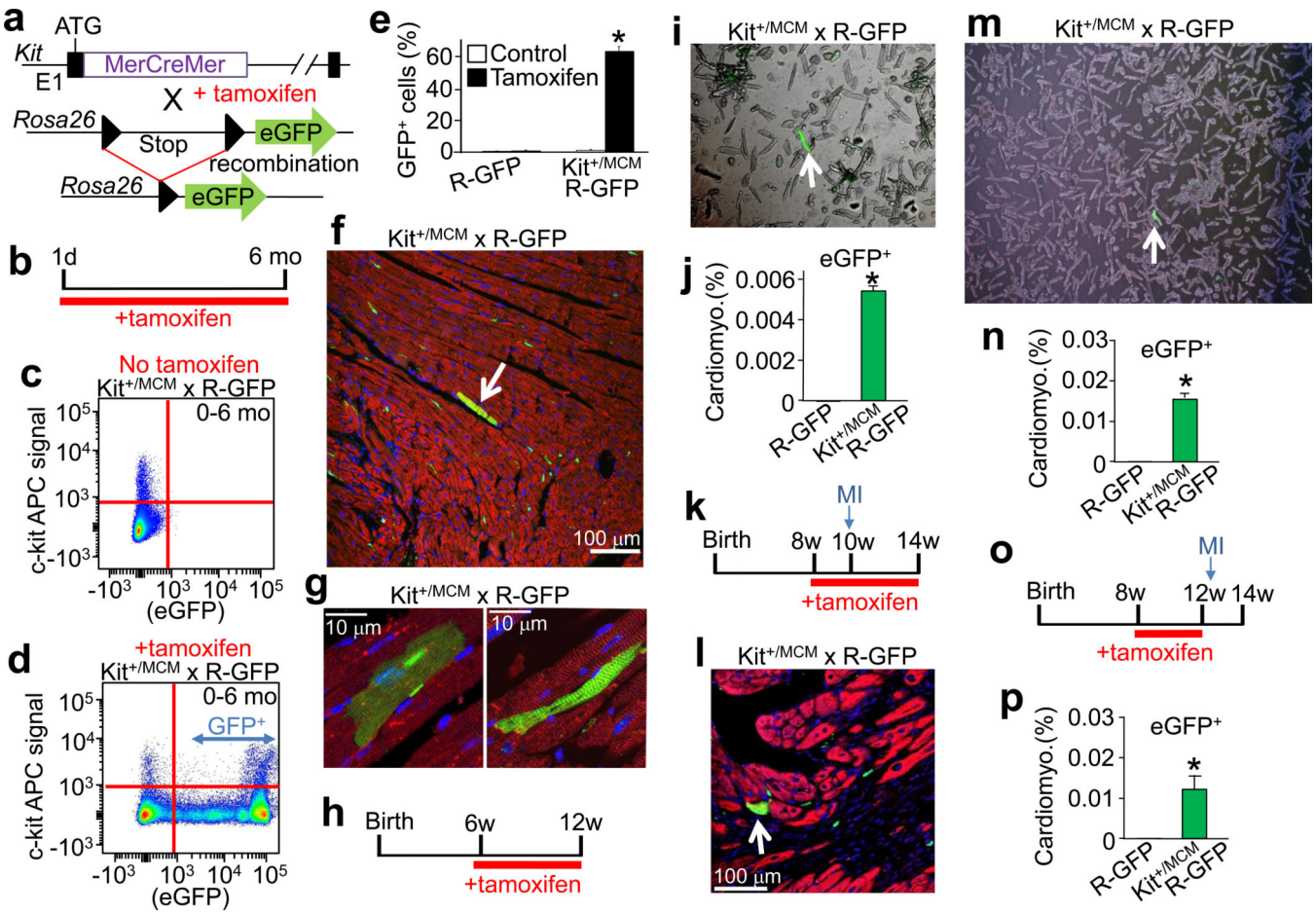

Figure 3. Inducible Cre expression from the *Kit* locus shows limited adult cardiomyocyte formation

a, Genetic cross between Kit$^{+/MCM}$ and R-GFP reporter mice to lineage trace c-kit expressing cells when tamoxifen is present. b, Schematic showing tamoxifen treatment between day 1 and 6 months of age (panels **c–g**). **c, d,** Representative FACS plots with c-kit antibody (APC) vs eGFP from bone marrow of Kit$^{+/MCM}$ × R-GFP mice without (**c**) or with tamoxifen (**d**). **e,** FACS quantification of eGFP^{+} cells from bone marrow of these mice (n=2 mice for R-GFP and n=4 for Kit$^{+/MCM}$ × R-GFP). *p<0.05 vs R-GFP. **f, g,** Representative heart sections from Kit^{+MCM} × R-GFP mice showing c-kit^{+} lineage cells in green and cardiomyocytes in red (desmin antibody). White arrow indicates eGFP^{+} adult cardiomyocyte. **h,i,j,** Tamoxifen treatment of Kit$^{+/MCM}$ × R-GFP mice between 6 – 12 weeks of age followed by disassociation of cells from the hearts of these mice in **h** (white arrow shows rare cardiomyocyte) that is quantified in **j** (127,284 cardiomyocytes across 2 hearts, 7 were eGFP^{+},*P<0.05 vs R-GFP). **k,l,m,n,** Tamoxifen treatment of Kit^{+MCM} × R-GFP mice between 8 and 14 weeks of age with myocardial infarction (MI) on week 10. **l,** Immunohistological heart section for desmin (red) and eGFP (green) with nuclei in blue (arrow shows a cardiomyocyte from the c-kit^{+} lineage). **m, n,** Disassociated cardiomyocytes show rare but definitive myocyte labeling (white arrow), which was quantified in **n** (225,760 cardiomyocytes from 2 MI hearts, 37 were eGFP^{+},*P<0.05 vs R-GFP). **o,p,** Tamoxifen treatment between 8 – 12 weeks of age with MI injury occurring 3 days after tamoxifen

cessation. **p**, Quantitation of $eGFP^+$ cardiomyocytes from histological images taken from 2 hearts of these mice. $eGFP^+$ cardiomyocytes were quantified as a percentage of the total cardiomyocyte fraction in >50 histological sections across the entire heart. *P<0.05 vs R-GFP. All error bars represent s.e.m.

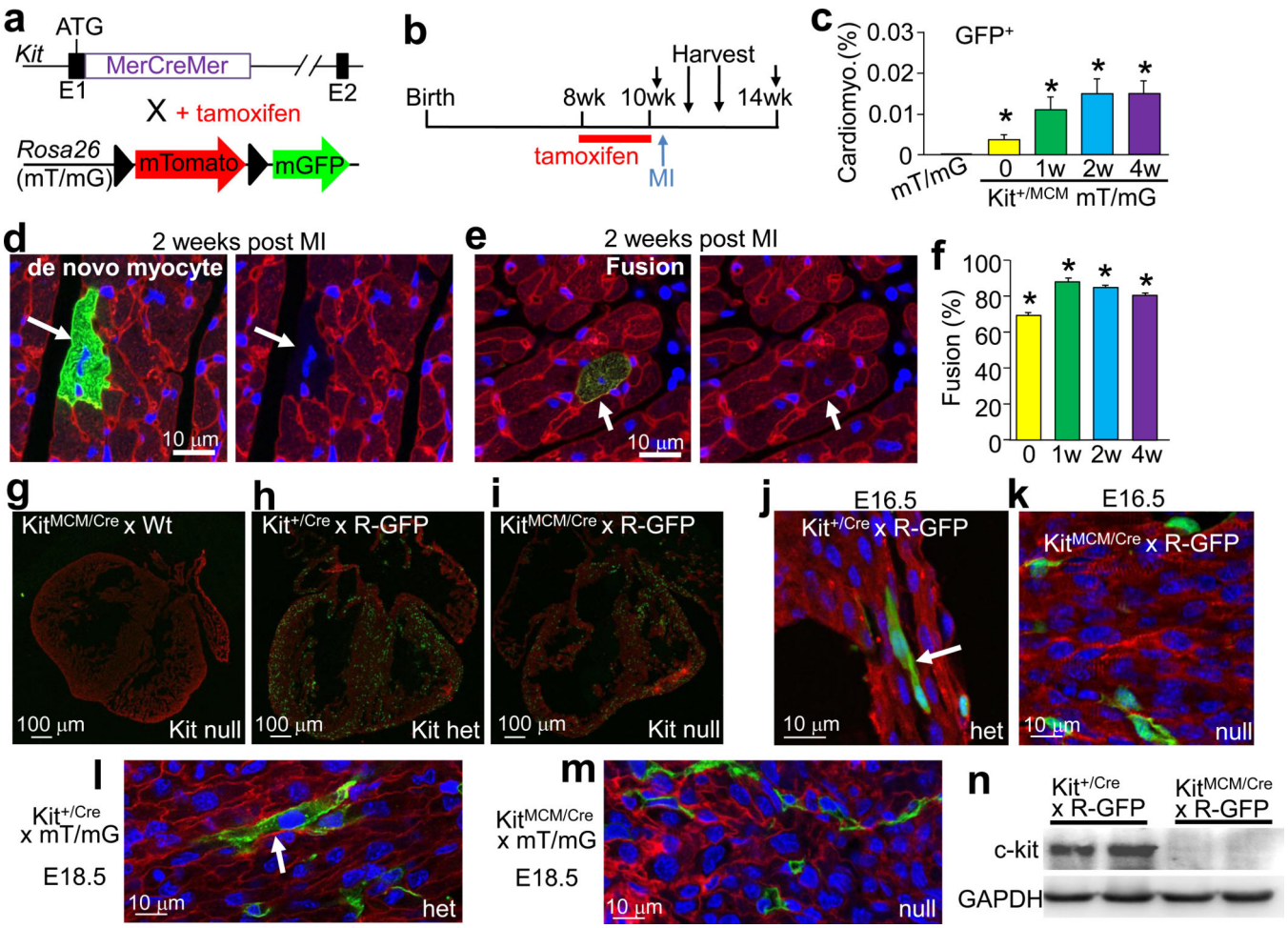

Figure 4.

Assessment of fusion versus de novo cardiomyocyte formation in the heart. **a,** Genetic strategy in which $Kit^{+/MCM}$ mice were crossed with *Rosa26* targeted mice containing the membrane targeted tdTomato/eGFP (mT/mG) reporter. **b,c,d,e,f,** Tamoxifen was given to Kit^{+MCM} × mT/mG mice between 8 and 10 weeks, followed 3 days later by MI injury. **c,** Quantitation across >50 histological sections of all $eGFP^{+}$ expressing cardiomyocytes before MI (n=4 hearts) and 1 (n=4 hearts), 2 (n=5 hearts) and 4 (n=3 hearts) weeks after MI injury. Error bars represent s.e.m., *P<0.05 vs mT/mG. **d,** Example of a c-kit lineage derived de novo cardiomyocyte in which membrane-eGFP (green, left) is expressed and tdTomato fluorescence (red, right) is lost. **e,** Example of $eGFP^{+}$ cardiomyocyte (green) that still contains endogenous membrane-tdTomato fluorescence (red), indicating fusion. Nuclei are stained blue. **f**, Quantitation of fusion percentage. *P<0.05 vs mT/mG. **g, h, i,** Immunohistological images from embryonic (E) day 16.5 mouse hearts that are either $Kit^{+/Cre}$ × R-GFP (het [**h**]), $Kit^{MCM/Cre}$ × R-GFP (null, [**i**]) or $Kit^{MCM/Cre}$ (null, no reporter, [**g**]). Red staining is α-actinin and green is eGFP. **j**, Higher magnification image from **h**, showing a definitive $eGFP^{+}$ cardiomyocyte (arrow). **k**, Higher magnification image from **i**, which shows only $eGFP^{+}$ non-myocytes in *Kit* null hearts. **l, m,** Histological heart images from E18.5 $Kit^{+/Cre}$ (het) and $Kit^{MCM/Cre}$ (null) embryos containing the mT/mG reporter,

again only the heterozygotes show examples of $eGFP^{+}$ cardiomyocytes (arrow). **n**, Western blot showing loss of c-kit protein in $Kit^{MCM/Cre}$ embryos (nulls) versus heterozygous controls.